

# A high definition look at the NF-Y regulome reveals genome-wide associations with selected transcription factors

Diletta Dolfini<sup>1</sup>, Federico Zambelli<sup>1,2</sup>, Maurizio Pedrazzoli<sup>1</sup>, Roberto Mantovani<sup>1</sup> and Giulio Pavese<sup>1,\*</sup>

<sup>1</sup>Dipartimento di Bioscienze, Università degli Studi di Milano, Milano, Via Celoria 26, 20133, Italy and <sup>2</sup>Istituto di Biomembrane e Bioenergetica, Consiglio Nazionale delle Ricerche, Bari, Via Amendola 165/A, 70126, Italy

Received January 28, 2015; Revised February 08, 2016; Accepted February 09, 2016

## ABSTRACT

**NF-Y is a trimeric transcription factor (TF), binding the CCAAT box element, for which several results suggest a pioneering role in activation of transcription. In this work, we integrated 380 ENCODE ChIP-Seq experiments for 154 TFs and cofactors with sequence analysis, protein–protein interactions and RNA profiling data, in order to identify genome-wide regulatory modules resulting from the co-association of NF-Y with other TFs. We identified three main degrees of co-association with NF-Y for sequence-specific TFs. In the most relevant one, we found TFs having a significant overlap with NF-Y in their DNA binding loci, some with a precise spacing of binding sites with respect to the CCAAT box, others (FOS, Sp1/2, RFX5, IRF3, PBX3) mostly lacking their canonical binding site and bound to arrays of well spaced CCAAT boxes. As expected, NF-Y binding also correlates with RNA Pol II General TFs and with subunits of complexes involved in the control of H3K4 methylations. Co-association patterns are confirmed by protein–protein interactions, and correspond to specific functional categorizations and expression level changes of target genes following NF-Y inactivation. These data define genome-wide rules for the organization of NF-Y-centered regulatory modules, supporting a model of distinct categorization and synergy with well defined sets of TFs.**

## INTRODUCTION

The mechanisms of transcriptional activation by RNA polymerase II involve a complex set of events, that include the binding of transcription factors (TFs) to specific DNA sequences in promoters and enhancers (TF binding sites, TFBSs), the recruitment of non DNA-binding co-

activators, many of which have chromatin-modifying activities, and the association of general transcription factors (GTFs). The process is influenced by local patterns of histone modifications, which, in turn, are ‘written’ and ‘read’ by enzymes recruited by TFs and cofactors. A central theme in modern biology and genetics is, therefore, the dissection of this highly complex process in molecularly identifiable units or modules, each responsible for a precise function and/or the regulation of specific sets of genes.

The CCAAT box, one of the first cis-acting promoter elements discovered, was identified in numerous studies over the past decade as a widespread feature of mammalian promoters (1–5), and indeed among one of the few ‘driver’ or ‘cardinal’ TFBSs in human (6–8) and mouse (9) regulatory regions. Its location in promoters is relatively precise, from 60 to 100 base pairs upstream of transcription start sites (TSSs), and it is found in diverse classes of genes, many of which belong to inducible systems, such as heat shock, endoplasmic reticulum (ER) stress, DNA-damage, cell-cycle (10) and also in genes overexpressed in cancer cells, particularly in the most aggressive ones (11–14).

By employing *in vitro* biochemical and *in vivo* genomic assays, the transcription factor NF-Y (also termed CBF) was found to be the primary factor with CCAAT-binding activity (15). NF-Y is a trimeric protein formed by the evolutionarily conserved subunits NF-YA, NF-YB and NF-YC, whose sequence-specific DNA recognition has been recently documented by structural studies (16,17). The vital physiological importance of NF-Y was documented in models of NF-YA knockout mice, in embryos (18) and in conditional experiments in hepatic, hematopoietic, neuronal and adipocyte systems (19–22). The biology of the three subunits is complex, both because NF-YA and NF-YC have multiple splicing isoforms with different function and expression levels in different tissues, and because the subunits are subject to post-translational modifications (PTMs), such as phosphorylations, acetylations and ubiquitinations (23).

\*To whom correspondence should be addressed. Tel: +39 02 503 14884; Email: giulio.pavese@unimi.it

A comprehensive effort to characterize genome-wide TFs binding and interplay in the human genome has been carried out by the ENCODE consortium (24,25), through hundreds of ChIP-Seq experiments in several different cell lines. The analysis of the massive amount of data produced has been so far extremely informative, confirming on one hand the specificity of many TFs for the binding motifs previously identified *in vitro*, and allowing on the other for the identification of novel ones (26–28). At the same time, however, it has detailed a more complex picture, in which many TFs appear to be bound to genomic locations devoid of their canonical target sequence, likely via protein–protein interactions with other sequence-specific TFs (26,29).

The identification of NF-Y genomic bound regions within the ENCODE project was performed by ChIP-Seq for NF-YA and NF-YB in the three ENCODE Tier-1 cell lines (K562, HeLa-S3 and GM12878), with an initial partial characterization of its relationships with 78 other TFs in K562 cells (30). The data confirmed the general requirement for the CCAAT binding motif, and also a widespread binding to enhancers, previously observed in more limited ChIP on chip experiments (31,32). Additional relevant conclusions concerned the association of NF-Y to LTR repetitive sequences, the precise arrangement of binding sites with respect to some E-box binding TFs, and the widespread presence of FOS to NF-Y bound regions devoid of canonical AP1 sites. The binding to LTR regions and correlation with some TFs were also reported in other studies (26,29).

The association of NF-Y to nucleosome-dense regions devoid of open chromatin common histone PTMs, peculiar among ENCODE TFs, suggested that NF-Y is a ‘pioneer’ TF driving the initial opening of chromatin territories for the build-up of competent transcription complexes. This conclusion was further supported by independent studies: (i) the analysis of DNase I hypersensitive sites through unbiased machine-learning methods, coupled with ChIPs and functional *in vivo* experiments (33); (ii) ChIP-Seq and RNAi analysis of the three NF-Y subunits in mES cells indicated that NF-Y promotes chromatin accessibility to master TFs like OCT4, SOX2 and NANOG in enhancers of developmentally controlled genes (34); (iii) The 3D structure of the trimer in complex with DNA (17) detailed two important features in line with a pioneering role: first, the overall area of DNA contacts is rather large (25/28 bps) for a TF, with sequence-specific recognition by NF-YA in the CCAAT minor groove area, leaving neighboring major grooves, generally the recognition points of DNA-binding TFs, open for binding; second, NF-Y is able to bend DNA – acting as an ‘architectural’ TF that shapes the three-dimensional arrangement of the promoter, bringing distal TFs closer to the general transcription machinery; (iv) Elimination of NF-Y binding by RNAi of one of its subunits or overexpression of a Dominant Negative NF-YA mutant, is detrimental for *in vivo* promoter recruitment of a disparate set of TFs and cofactors (35–47).

The near-ubiquitous pattern of expression of NF-Y subunits and widespread occurrence of CCAAT boxes in promoters might suggest a model whereby NF-Y could serve a pioneering role to most, or all, TFs in any specific CCAAT promoter. On the other hand, past individual dissections of promoters and TF–TF interactions would argue in favor

of a more specific interplay, taking place only with selected classes of TFs and co-factors.

Reconstructing the genomic interplay map of NF-Y with other TFs is essential in order to rationalize and integrate this sketchy plot, assembled so far by using pieces of information on single TFs and promoters. For this task, in this work we systematically analyzed the enrichment for NF-Y sites in the genomic loci bound by 154 TFs tested in the ENCODE Project in K562, HeLa-S3 and GM12878 cell lines, for a total of about 380 different ChIP-Seq experiments, identifying a subset of TFs which tend to bind *in vivo* throughout the genome the same DNA regions of NF-Y. Among these, we also singled out several cases in which the binding of NF-Y and the other TF requires a precise arrangement of binding sites on DNA. We then further integrated these observations with protein–protein interaction data, and provided a functional characterization of the genes targeted by the different associations, as well as the respective expression profiles after NF-Y-inactivation.

## MATERIALS AND METHODS

### Motif enrichment analysis

We considered all ENCODE ChIP-Seq data sets of K562, GM12878 and HeLa-S3, i.e. cell lines for which NF-YA and NF-YB ChIP-Seq experiments were available. Peak coordinates were retrieved from the UCSC Genome Browser database (48), and regions around the peak summits submitted to PscanChIP (49) version 1.0, for assessing the enrichment of the CCAAT box. Differently from other motif enrichment analysis tools, PscanChIP evaluates motif enrichment in peak regions from ChIP-Seq experiments with two different criteria: global or local enrichment:

*Global enrichment* is assessed according to a genomic background, and motifs found to be enriched according to this measure are over-represented in the selected regions with respect to the rest of the genome accessible to TF binding. Thus, they tend to be found in the genome prevalently in correspondence to the binding regions of the TF investigated. Hence, a motif with significant global enrichment could correspond to the actual binding site of the TF (usually the most significant one), or binding sites of other TFs which show a clear genome-wide tendency to bind in association with it.

*Local enrichment*, instead, evaluates whether, whenever an instance of the motif is found in the neighborhood of a peak region, it is more likely to be close to the peak summit—where TF binding usually takes place—or not. Globally enriched motifs are usually enriched also locally. On the other hand, motifs enriched only according to this measure—and not globally—correspond to binding sites for TFs which tend to bind in close proximity of the TF for which the experiment was performed, but in a limited subset of regions, and not as a genome wide rule.

In both cases, enrichment is evaluated according to a Bonferroni-corrected *P*-value. To highlight only the strongest candidates, we deemed to be significantly enriched for the CCAAT box those data sets where the *P*-value was lower than  $10^{-10}$  for either criterion. Since for the evaluation of global enrichment PscanChIP employs cell-specific background expected values, K562 data were analyzed with

the respective PscanChIP background, while for HeLa-S3 and GM12878 we employed the ‘mixed’ background that is suitable for cell lines for which data for computing the background values were not available. As descriptor of the CCAAT box motif we employed the JASPAR (50) matrix with ID MA0060.1. This matrix was originally described by one of us (51), and later confirmed by ChIP-chip (10) and *de novo* motif discovery in diverse sources of ChIP-Seq data (26,28,30,34,40,52). Factors with a significant enrichment for CCAAT boxes in their peaks were then submitted to further analyses in additional cell lines in which NF-Y experiments were not performed by ENCODE. The full data set analyzed, together with the complete PscanChIP results are available as Supplementary Table S1.

The PscanChIP tool contains also a module able to evaluate any positional bias for motifs within peak regions, in two different ways: (i) preferential positioning of a motif with respect to the peak summit, another indicator that the motif might be essential for the recruitment to DNA of the TF investigated, and (ii) preferential relative positioning of two different motifs, or two instances of the same motif, possible indicator of co-operative binding of two different TF, or a single TF binding as a dimer. In both cases, PscanChIP associates with any positional bias a *P*-value computed assuming a uniform distribution of the distance between motif instances. Hence, in data sets with significant enrichment for the CCAAT box, preferential distances among pairs of CCAAT boxes, or the CCAAT box and the binding sites of the other TFs, were also assessed by analyzing the regions bound both by NF-Y and each of the TFs, and reported to be significant if the associated *P*-value was lower than  $10^{-10}$ .

### Genome-wide peak co-association

Since finding the CCAAT box motif enriched in peaks for TFs other than NF-Y, by itself, is no guarantee of *in vivo* NF-Y binding, we also determined, for each data set, the actual association of the TF studied with NF-Y by crossing its ChIP-Seq peak coordinates with the ones of both NF-YA and NF-YB in the same cell line, and assessing if the overlap could be considered significant, i.e. widespread genome-wide. Pairwise overlap between two ChIP-Seq data sets was defined by considering two peaks as ‘overlapping’ if the respective summits fell within 150 bps from one another. Starting from this definition we defined a co-association score able to capture the significance of the overlap. Given two data sets, with *m* and *n* peaks respectively, and *k* peaks considered to be overlapping according to the criterion just described, we assumed that across the genome there exists a number *N* of regions of 150 bps available for TF binding. Then, we assessed the probability of having by chance *k* peak regions out of *N* in common between the two TFs with a Fisher Exact Test with parameters *k* (the number of overlapping peak regions), *n*, *m*, (the number of peaks in the two data sets compared, respectively) and *N*.

The problem was to define a suitable value for *N*, which is a key value for the *P*-values produced. We considered taking into account the whole genome not to be a correct choice, since in every cell line or condition most of it is not accessible to TF binding. Thus, as in a previous work (49), we used as an estimate for *N* the number of chromatin accessible re-

gions, identified by DNaseI ‘hyperaccessibility’ or ‘hypersensitivity’, which is indeed a feature of active cis-regulatory sequences. For this, we considered ENCODE DNaseI Digital Genomic Footprinting regions available at the UCSC genome browser database (48), which are exactly 150 bps long. The number is clearly variable in different cell lines, but ranges from 200 000 to 300 000 in all the cell lines available. In this work, we employed *N* = 250 000 for all the cell lines studied. Starting from the *P*-value, *P* returned by the Fisher test we defined the co-association score as  $-\log_{10} P$  if *k* was greater than the expected value,  $\log_{10} P$  otherwise. Once again, in order to single out the strongest candidates corresponding to genome-wide co-associations, and not only to co-associations derived from, e.g. the fact that TFs tend to bind promoters and/or enhancers, we considered two ChIP-Seq experiments to be ‘significantly overlapping’ if the resulting co-association score was > 100 for both NF-YA and NF-YB.

For the identification of more complex regulatory modules, we also computed pairwise co-associations *within* NF-YB peaks for pairs of TFs in a similar fashion, by counting the number *k* of NF-YB summits that in turn contained a summit for both TFs within 150 bps, but in this case defining *n* and *m* as the number of summits for each TF located within 150 bps from a NF-YB summit, and setting for the Fisher Exact Test *N* as the overall number of NF-YB peaks. Co-association matrices and heatmaps were obtained for each cell line by performing a hierarchical clustering on co-association scores, using Pearson correlation as distance and UPGMC as clustering method, as implemented in the *hclust* R function, in order to identify groups of TFs clustering together when binding in association with NF-Y.

### Lentivirus transductions, Western blots and ChIPs

The shRNA expressing (Scramble and shNF-YB) and packaging (VSVG and pCMV-dR8.74) plasmids were transfected in HEK293T cells to obtain lentiviruses. Lentivirus-containing supernatant was collected 48 h after transfections, filtered and frozen at  $-80^{\circ}\text{C}$ . HeLa Cells ( $30 \times 10^6$ ) were plated, infected with viral supernatants and harvested after 72 h. After fixation with formaldehyde (1% for 10'), crosslinked chromatin was sonicated (Bioruptor, Diagenode) to fragments of approximately 1/1.5 kbp in length, as checked by Agarose gel electrophoresis. ChIP assays were performed as described (35) with 5  $\mu\text{g}$  of the following antibodies: anti-FLAG (Sigma-F3165), anti-NF-YB (GeneSpin), anti-ELK4 (Santa Cruz sc-13030), anti-E2F4 (Santa Cruz sc-1082) anti-CEBP/B (Santa Cruz sc-150). Immunoprecipitated DNAs were re-suspended in TE buffer and used for analysis by quantitative PCR.

From HeLa cells infected in parallel with lentiviral supernatants, total extracts were re-suspended in SDS buffer and Western blots performed according to standard procedures, incubation overnight with the indicated primary antibodies and for 2 h with a peroxidase conjugated secondary antibody (Sigma). Digital images were collected by Chemidoc MP (Biorad).

## Quantitative PCR analysis

Quantitative real time PCR (RT-PCR) was performed using SYBR Green (Biorad Soadvance mix) in IQ5 Biorad PCR machine. Primers (listed in Supplementary Table S7) were designed with Primer3 software, to amplify genomic regions of 80–150 bp. Relative enrichment was calculated as  $2^{\text{DCtx}} - 2^{\text{DCtb}}$ , where  $\text{DCtx} = (\text{Ct input} - \text{Ct sample})$  and  $\text{DCtb} = (\text{Ct input} - \text{Ct control antibody})$ . Resulting values were normalized with respect to a negative locus. Data are shown as percentage of difference in TFs binding in shNF-YB-treated cells compared to shScramble-treated cells. Values are the means of two independent biological replicates and qPCR performed in triplicates.

## Protein–protein interaction and expression data

We retrieved protein–protein interaction data from BioGrid version 3.4 (53), integrating them with available literature on NF-Y (28,54–59), in order to associate positional bias of binding sites with interactions at the protein level of corresponding TFs. Transcription profiling data after NF-YA inactivation by shRNA, available for HeLa-S3 cells were retrieved from (30) (GEO accession GSE40215). As in the original work, arrays were RMA normalized, gene expression levels calculated, differential expression determined and probes annotated using the R Bioconductor packages *affy* and *limma*. We defined as up-regulated and down-regulated those genes with fold change above 1.3 and  $\text{FDR} < 0.05$ . Gene ontology enrichment was computed using DAVID version 6.5.

## RESULTS

### NF-Y has genome-wide partnerships with selected transcription factors

The workflow of the analysis is shown in Figure 1. Enrichment analysis for the CCAAT box motif in ChIP-Seq experiments for other TFs was based on three criteria, corresponding to the different modes of enrichment PscanChIP is able to identify, as described in the Materials and Methods section: (i) NF-Y was identified by PscanChIP as having the ‘primary binding site’ in the peak regions, that is, the CCAAT box was singled out as the motif with highest ‘global’ enrichment in the regions; in this case, the CCAAT box could be considered as the main sequence element responsible for the binding to DNA of the TF studied in the ChIP-Seq experiment (highlighted in red in Table 1). Note that this does not imply that the TF binds to CCAAT directly, but it suggests that a CCAAT-bound NF-Y might be mediating recruitment. (ii) NF-Y was scored as ‘secondary binding site’, i.e. it was significantly enriched at the global level according to PscanChIP, but was not the most enriched one, hinting at a widespread co-operative binding of NF-Y with the IP’ed TF, which is bound to its expected binding motif (highlighted in orange in Table 1). (iii) NF-Y was found to have only significant ‘local’ enrichment, hinting to close binding of NF-Y and the IP’ed TF, but limited to a subset of genomic regions not large enough to consider the phenomenon as a ‘general rule’ (highlighted in light green in Table 1).

The analysis on the peak regions for 154 ENCODE TFs available in K562, HeLa-S3 and GM12878 cell lines returned 33 factors, mostly sequence-specific TFs, with significant enrichment of CCAAT box in their ChIP-Seq bound regions in at least one cell line. The list is shown in Table 1. Notably, some of the data sets had the CCAAT box as ‘primary’ binding site. Indeed, independent genome-wide studies not linked to ENCODE already reported enrichment for NF-Y binding sites in the bound regions of ATF3 in HCT116 and LNCaP cells (60), Sp2 in HEK293 and mouse MEF cells (61,47), E2F4 in B cells GM06990 (62).

We then complemented the motif enrichment analysis by evaluating the co-occurrence of peak summits of NF-YB with those of each of the 33 TFs (see Materials and Methods and Supplementary Table S2). The results are also summarized in Table 1, with the percentage of peaks of each experiment sharing NF-YB summits in close proximity (the percentage column). The association identified by motif analysis was confirmed for nearly all the factors (29 out of 33), that had a significant overlap of their peaks with those of NF-Y, and therefore the CCAAT boxes found to be enriched are actually bound by NF-Y *in vivo*. We can also observe how the percentage of peaks overlapping NF-Y tends to be lower for those TFs with ‘local’ enrichment for the CCAAT box, while with ‘global’ CCAAT enrichment the overlap is usually more widespread. The four exceptions, for which the co-association score vice versa pointed to ‘significantly low’ overlap, were CTCF, the two associated subunits RAD21 and SMC3, together part of the cohesin complex and CDP (CCAAT Displacement Protein). For these, the enrichment found by PscanChIP was ‘local’, and overlap with NF-Y peaks marginal and not significant. The presence of CCAAT boxes with low peak association might reflect mutually exclusive binding: indeed, this was one of the original features described *in vitro* for CDP (63). It should also be noted that good NF-Y/CTCF intersections were recently reported in mES cells induced to neuronal differentiation, but not in growing cells (34), suggesting that the NF-Y/Cohesin interplay might be cell-type specific or related to the status of the cell (growing versus differentiated).

To characterize better the results obtained for each of the TFs listed in Table 1, and to assess whether the CCAAT box motif could be considered the primary binding motif in case of global enrichment, we ran a second round of PscanChIP experiments, focusing on the subset of TF-bound regions overlapping with NF-YB peaks, as defined in the previous step, thus bound *in vivo* both by NF-Y and the individual TF. Quite naturally, all the factors with CCAAT box globally enriched in their peaks had it also in these subsets, either as the primary ‘global’ binding motif or a secondary one, preceded by the binding site for the TF (summarized in column ‘Pos overlap’ in Table 1, where ‘1’ indicates the CCAAT box as primary binding site and ‘2’ secondary, respectively). For FOS, that in HeLa-S3 had the CCAAT box preceded in the ranking of enrichment motifs only by the canonical AP1 motif, the CCAAT box is confirmed as the primary motif in the overlapping regions in all cell lines, with no enrichment found for AP1, which vice versa can be found as primary site in regions co-bound by FOS and JUN, but not NF-Y. Indeed, AP1 and CCAAT box sites had been previously shown to co-exist with a precise spacing only in

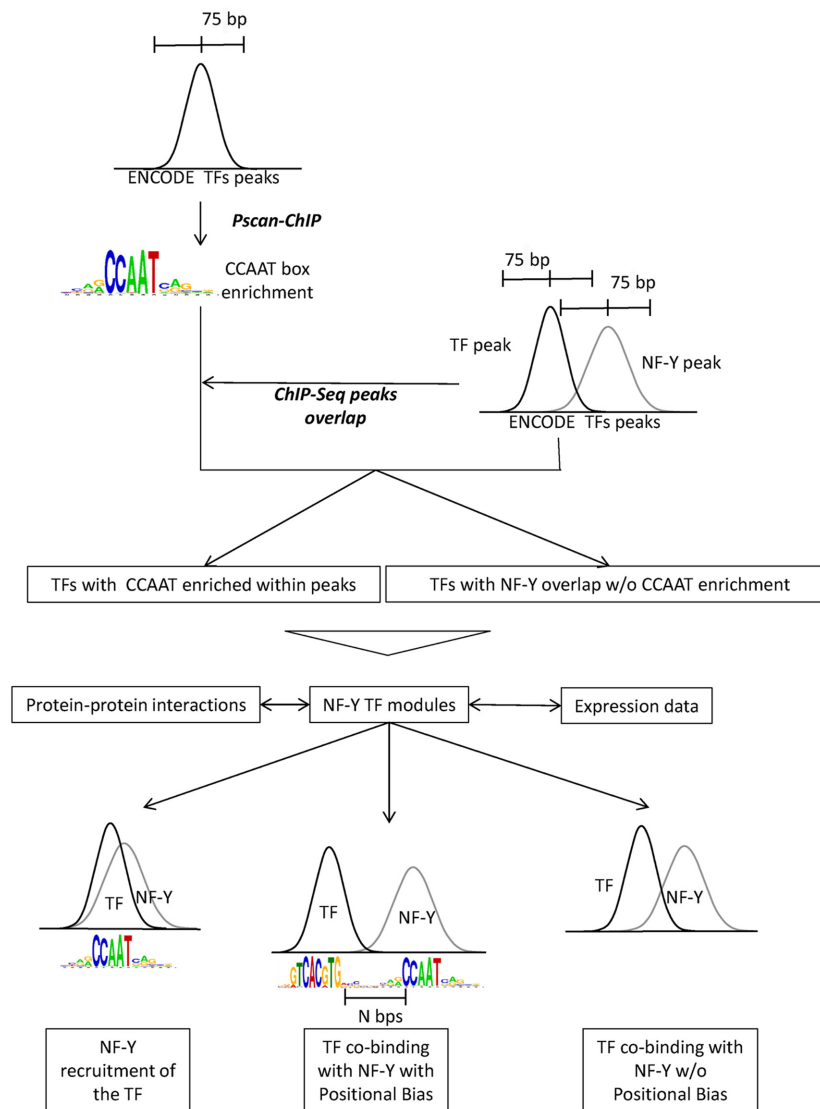


**Figure 1.** Analysis workflow. The whole set of TFs and co-factors with ChIP-Seq data in ENCODE (K562, HeLa-S3 and GM12878) were analyzed with PscanChIP to evaluate CCAAT enrichment. In parallel, we calculated the overlap of peaks for each of the 154 ENCODE factors from the three cell lines with NF-Y peaks. The NF-Y modules derived from these data were integrated by two sets of data: protein–protein interactions, taken from the BIOGRID database and gene expression data after NF-YA-inactivation in HeLa-S3. Three resulting modes of NF-Y/TF interactions are shown at the bottom: NF-Y-mediated binding of a TF, in the absence of a specific TF recognition sequence (Left); co-binding of NF-Y and a TF, with positional constraints between the respective binding sites (Center); TF co-binding with NF-Y without any precise arrangement of sites (Right).

a limited set of regions, bound by both FOS and NF-Y, corresponding to LTR repeats (30,49). These findings point to two different main modes of genome targeting for FOS, one mediated by NF-Y/CCAAT, and another through the canonical AP1 motif. The same argument holds for CHD2 and RFX5, where the CCAAT box emerges as the primary motif in regions bound by NF-Y, with other motifs (CTCF for CHD2, the RFX motif for RFX5) not enriched in the regions bound together with NF-Y and becoming instead the main one when NF-Y is absent. All in all, the CCAAT box is the main motif found in regions bound by NF-Y and FOS, CHD2, IRF3, RFX5, PBX3, Sp1 and Sp2. All the other CCAAT-enriched TFs had instead the respective canonical motif as the most enriched also in the regions co-bound by NF-Y. For the TFs with ‘local’ enrichment for the

CCAAT box, a secondary CCAAT enrichment in the peaks that overlapped NF-Y was confirmed. The sole exception was CoREST, for which the CCAAT box was found to be the most enriched motif in the presence of NF-Y binding.

We also computed for all the data sets whether there was any positional bias among binding sites, i.e. whether the CCAAT box and the motif known to be bound by the TF presented a preferential spacing in the co-bound regions, or whether more than one CCAAT box could be present in the regions, since NF-Y is known to bind also multiple instances of its binding site. Indeed, most had a significant positional bias, as scored by PscanChIP and described in the Materials and Methods section (see ‘Pos bias’ column in Table 1, and section ‘DNA organization of binding sites’ further on). Finally, for the TFs listed in Table 1, we extended

Table 1. Proteins whose *in vivo* binding sites are enriched in CCAAT boxes

TFs	GM12878				HeLa-S3				K562				hESCs				HepG2	A549	IMR90	Huvec	SH-N-SH	MCF7	HCT116	HECC1
	CCAAT Enriched	CCAAT in overlap	Pos Bias	%	CCAAT Enriched	CCAAT in overlap	Pos Bias	%	CCAAT Enriched	CCAAT in overlap	Pos Bias	%	CCAAT Enriched	CCAAT Enriched	CCAAT Enriched	CCAAT Enriched	CCAAT Enriched	CCAAT Enriched	CCAAT Enriched	CCAAT Enriched	CCAAT Enriched	CCAAT Enriched		
ARID3A	NO DATA				NO DATA							5	ARID3A	NO DATA		NO DATA	NO DATA	NO DATA	NO DATA	NO DATA	NO DATA	NO DATA		
ATF1	NO DATA				NO DATA							7	ATF1	NO DATA	NO DATA	NO DATA	NO DATA	NO DATA	NO DATA	NO DATA	NO DATA	NO DATA		
ATF3	no			23	NO DATA							25	ATF3			no	NO DATA	NO DATA	NO DATA	NO DATA	NO DATA	NO DATA		
BRCA1	no			25		2		16	NO DATA				BRCA1	no	no	NO DATA	NO DATA	NO DATA	NO DATA	NO DATA	NO DATA	NO DATA		
CDP				8	NO DATA							6	CDP	NO DATA	NO DATA	NO DATA	NO DATA	NO DATA	NO DATA	NO DATA	NO DATA	NO DATA		
CEBPB	no			8				Yes 3			Yes 3	3	CEBPB					NO DATA	NO DATA	NO DATA	NO DATA	NO DATA		
C-FOS		1	Yes	89		1	Yes	12		1	Yes	48	C-FOS	NO DATA	NO DATA	NO DATA	NO DATA		NO DATA	NO DATA	NO DATA	NO DATA		
CHD2		2	Yes	23		2	Yes	18		2	Yes	12	CHD2			NO DATA	NO DATA	NO DATA	NO DATA	NO DATA	NO DATA	NO DATA		
COREST	no			16				10			Yes 4	4	COREST	NO DATA	no	NO DATA	no	NO DATA	NO DATA	NO DATA	NO DATA	NO DATA		
CTCF				5				1				2	CTCF											
E2F4		2		35		2		28		2		20	E2F4	NO DATA	NO DATA	NO DATA	NO DATA	NO DATA	NO DATA	NO DATA	NO DATA	NO DATA		
ELF1				15	NO DATA							8	ELF1	NO DATA		no	NO DATA	NO DATA	NO DATA	NO DATA	NO DATA	NO DATA		
GABP	no			24	no			15				12	GABP	no	no	no	NO DATA	NO DATA	no	no	NO DATA	NO DATA		
HCFC1	NO DATA					2	Yes	40			Yes 8	8	HCFC1	NO DATA	NO DATA	NO DATA	NO DATA	NO DATA	NO DATA	NO DATA	NO DATA	NO DATA		
IRF3		1	Yes	19		1	Yes	89	NO DATA				IRF3	NO DATA		NO DATA	NO DATA	NO DATA	NO DATA	NO DATA	NO DATA	NO DATA		
JUND	no			6			Yes	4			Yes 4	4	JUND	no		NO DATA	NO DATA	NO DATA		NO DATA	NO DATA	NO DATA		
MAFF	NO DATA				NO DATA						Yes 2	2	MAFF	NO DATA		NO DATA	NO DATA	NO DATA	NO DATA	NO DATA	NO DATA	NO DATA		
MAFK	no			1			Yes	4			Yes 3	3	MAFK			NO DATA	NO DATA	NO DATA	NO DATA	NO DATA	NO DATA	NO DATA		
MAX	no			18				15			Yes 58	58	MAX		no	NO DATA	NO DATA	NO DATA	no	no	no	NO DATA		
NFE2		2		17	NO DATA				no			6	NFE2	NO DATA	NO DATA	NO DATA	NO DATA	NO DATA	NO DATA	NO DATA	NO DATA	NO DATA		
PBX3		2	Yes	22	NO DATA				NO DATA				PBX3	NO DATA	NO DATA	no	NO DATA	NO DATA	no	NO DATA	NO DATA	NO DATA		
RAD21			Yes	2			Yes	2			Yes 1	1	RAD21	NO DATA	NO DATA	NO DATA	NO DATA	NO DATA	NO DATA	NO DATA	NO DATA	NO DATA		
RFX5		1	Yes	47		1	Yes	14		1	Yes	6	RFX5			NO DATA	NO DATA	NO DATA		NO DATA	NO DATA	NO DATA		
RUNX3			Yes	6	NO DATA				NO DATA				RUNX3	NO DATA	NO DATA	NO DATA	NO DATA	NO DATA	NO DATA	NO DATA	NO DATA	NO DATA		
SIX5		2		27	NO DATA							17	SIX5		NO DATA	no	NO DATA	NO DATA	NO DATA	NO DATA	NO DATA	NO DATA		
SMC3			Yes	2			Yes	2			Yes 3	3	SMC3	NO DATA	NO DATA	NO DATA	NO DATA	NO DATA	NO DATA	NO DATA	NO DATA	NO DATA		
SP1		1	Yes	26	NO DATA					1	Yes	36	SP1			NO DATA	NO DATA	NO DATA	NO DATA	NO DATA	no	NO DATA		
SP2	NO DATA				NO DATA					1	Yes	61	SP2			NO DATA	NO DATA	NO DATA	NO DATA	NO DATA	NO DATA	NO DATA		
SRF				16	NO DATA				no			10	SRF			NO DATA	NO DATA	NO DATA	NO DATA	no	no	no		
TBP		2		20		2		13	no			10	TBP			NO DATA	NO DATA	NO DATA	NO DATA	NO DATA	NO DATA	NO DATA		
USF1		2	Yes	21	NO DATA					2	Yes	14	USF1			NO DATA	NO DATA	NO DATA		NO DATA	NO DATA	no		
USF2		2	Yes	21		2	Yes	12		2	Yes	19	USF2			NO DATA	NO DATA	NO DATA	NO DATA	NO DATA	NO DATA	NO DATA		
ZNF143			Yes	9	no			18			Yes 12	12	ZNF143		NO DATA	NO DATA	NO DATA	NO DATA	NO DATA	NO DATA	NO DATA	NO DATA		

Transcription factors and co-factors with significant enrichment for the CCAAT box near peak summits, in the three cell lines analyzed. Colors represent the enrichment mode found: red, CCAAT globally enriched as primary binding site; orange, CCAAT globally enriched as secondary binding site; light green, local enrichment; grey, no significant enrichment. 'NO DATA' indicates TF/cell line experiments not available in ENCODE data. For each TF/cell line pair, the 'CCAAT in Overlap' indicates whether the CCAAT box is the primary (1) or secondary (2) motif in the regions resulting bound by both NF-Y and the TF according to ChIP-Seq data. The presence of positional bias between the respective TFBSs is indicated in the 'Pos bias' column. The percentage of peaks for the TF overlapping with those of NF-Y is shown in the percentage column.

the analysis to all the available ENCODE ChIP-Seq experiments, in cell lines in which NF-Y binding data are missing. The results are also shown in Table 1: in general, most factors indeed showed ubiquitous CCAAT enrichment, but 12 were more cell-type restricted. Since ChIP-Seq for NF-Y in these cell lines are not available, further verification based on peak overlap was not possible.

From the results of the general peak overlap analysis, we also noticed 19 additional factors with a significant co-association with NF-YA and NF-YB peaks (and overlap > 10%), but no enrichment for CCAAT boxes in PscanChIP analysis, according to the stringent significance threshold we employed (Table 2 and Supplementary Table S2). We considered this group to be relevant for the following reasons: (i) The analysis of PscanChIP did anyway show mod-

erate enrichment of CCAAT boxes in the peaks of 8 TFs. (ii) A total of 10 out of the 11 sequence-specific TFs show significant overlap in more than one cell line, NRF1 and TAF1 in all three. (iii) There are additional members of families sharing common structural features, or subunits of complexes, of those found to be enriched for the CCAAT box (Table 1): E2F1/E2F6 (E2F4), EGR1 (Sp1/Sp2), ELK1/ELK4/ETS1 (ELF1/GABP/SRF), MYC/MXI1 (MAX/USF1/USF2), GTF2B, GTF2F1 and TAF1 (TBP). Therefore, we decided to add them to the downstream analyses performed.

**Table 2.** Other transcription factors and co-factors with significant overlap with NF-Y peaks, but without significant CCAAT box enrichment in the three cell lines analyzed

	GM12878			HELA			K562		
	Overlap Score YA	Overlap Score YB	% YB	Overlap Score YA	Overlap Score YB	% YB	Overlap Score YA	Overlap Score YB	% YB
E2F1	NO DATA			300	188	12	NO DATA		
E2F6	NO DATA			299	172	12	300	256	10
EGR1	126	259	13	NO DATA			no		
ELK1	219	300	22	300	300	18	no		
ELK4	NO DATA			300	293	14	NO DATA		
ETS1	no			NO DATA			275	140	10
GTF2B	NO DATA			NO DATA			300	300	20
GTF2F	NO DATA			300	300	12	296	108	11
MAZ	300	300	17	300	300	13	no		
MX11	300	300	17	300	300	14	no		
MYC	no			300	300	10	no		
NRF1	253	300	25	264	145	14	215	127	15
PLU1	NO DATA			NO DATA			300	229	10
PML	224	300	15	NO DATA			300	163	10
POU2F2	138	245	11	NO DATA			NO DATA		
SIN3A	253	300	17	NO DATA			205	118	9
TAF1	300	300	20	300	300	13	300	300	14
THAP1	NO DATA			NO DATA			211	135	15
YY1	137	134	9	NO DATA			171	115	12

Shaded boxes highlight TFs showing a moderate enrichment for CCAAT boxes, but below the thresholds considered for inclusion in Table 1. The percentage of NF-YB peaks overlapping with those of the indicated TF is shown for each TF.

### Different groups of factors co-associate with NF-Y locations

The different degrees of NF-Y co-association resulting from the combination of CCAAT enrichment and peak overlap analyses suggest that the TFs identified can be partitioned in three groups (summarized in Figure 2):

Group 1: TFs showing ‘global’ enrichment for the CCAAT box as primary or secondary motif, and overlap of the NF-Y/TF peaks >20% in at least one data set (red and orange in Table 1).

Group 2: TFs with only ‘local’ CCAAT box enrichment (Light green in Table 1) and/or lower peak overlap (<20%). Some factors do show ‘global’ enrichment in HepG2 or hESCs (ARID3A, ATF3, MAX and SRF) but inclusion in this group, rather than in the first, is due to the fact that it is impossible to verify the overlap with NF-Y peaks in these cells for the lack of ChIP-Seq data for NF-Y.

Group 3: all the factors with significant peak overlap but no significant enrichment for the CCAAT box (summarized in Table 2).

General transcription factors TAF1 (TFIID), GTF2B and GTF2F1 are in the third group, while TBP is in the first. TFs belonging to different DNA-binding domain families are variously grouped: (i) Basic-Leucine Zipper FOS, NFE2, ATF1/ATF3 (that have similar binding site matrices), C/EBPb, NRF1. (ii) Zinc Fingers Sp1, Sp2, Znf143, EGR1, MAZ. (iii) b-HLH TFs USF1/2 in Group 1, Max, MX11 in 2 and MYC in 3. (iv) TFs with ETS DNA-Binding Domain -ELF1, ELK1, ELK4, GABP, ETS1 and SRF- are split between Group 1 and 3. For FOS, IRF3, RFX5 and PBX3, all in Group 1, NF-Y is the primary site in the overlapping binding regions. All E2Fs family members tested by

TF Class	Group 1 Global CCAAT enrichment only Peaks overlap >20%	Group 2 Global or Local CCAAT enrichment Peaks overlap < 20%	Group 3 No CCAAT enrichment Peaks overlap > 10%
b-Zip	CFOS	JUND ATF1 ATF3 MAFF MAFK CEBPB NFE2	NRF1
b-HLH	USF1 USF2	MAX	MX11 MYC
ZNF	SP1 SP2	ZNF143	EGR1 MAZ
HD	SIX5 PBX3		POU2F2
E2F	E2F4		E2F1 E2F6
ETS		ELF1 GABP SRF	ELK1 ELK4 ETS1
Other	RFX5 IRF3	RUNX3 ARID3A	TCF7L2 THAP1 YY1
GTFs	TBP		GTF2B GTF2F TAF1
Cofactors	HCFC1 CHD2	COREST BRCA1	KDM5B SIN3A PML

**Figure 2.** Classification of factors in three groups according to enrichment of CCAAT boxes in their peak regions, and the overlap of the latter with both NF-YA and NF-YB peaks. Group 1 TFs have both global enrichment of CCAAT boxes and widespread overlap with NF-Y; Group 2 more limited enrichment and overlap; Group 3 TFs have significant overlap with both NF-YA and NF-YB but no significant CCAAT enrichment.

ENCODE (E2F4, E2F1 and E2F6) are present in one of the groups. As for cofactors, CHD2 and HCFC1 are in Group 1, and CoREST does have CCAAT as primary binding site in overlapping regions in Hela-S3, BRCA1 as secondary;

KDM5B, SIN3A and PML have significant overlap and are in Group 3.

### Multiple factor co-association modules

Given the TFs that showed significant co-association with NF-Y, we determined whether there were further multiple associations among them, that is, which ones tended to group together to form distinct regulatory modules when binding with NF-Y. Starting from regions bound by NF-YB, we computed for each pair of ENCODE TFs the number of peak summits pairs (one for TF) that were located within 150 bps from one another within the same NF-YB peak summit. In this way, we were able to compute a co-association score for each pair of TFs within NF-YB bound regions (see Materials and Methods), expressing the tendency of the two TFs to co-associate with NF-Y, and, in turn, to cluster together within the same regions when binding DNA together with NF-Y. We represented the results of this analysis with a matrix built according to the pairwise co-association scores (Supplementary Table S3).

In order to extend these co-associations to more than two pairwise TFs, we clustered the TF co-association matrix (see Materials and Methods), thus highlighting groups of multiple TFs that tend to co-localize when binding together with NF-Y. We present the results using heatmaps (Figure 3), where the intensity of color in cell  $(x,y)$  is proportional to the co-association score between transcription factors  $x$  and  $y$  within NF-YB peaks. We included in this analysis peaks of NF-YA, having very high overlap with those of NF-YB (30). The co-association of NF-YA with the other TFs in the heatmap reflects the degree of overlap of each of the latter with NF-Y itself (NF-YA<sup>+</sup> and NF-YB<sup>+</sup>): thus, clusters with the highest correlation with NF-YA are those that in turn have the strongest co-association with NF-YB and hence NF-Y in general.

In K562, where the largest number of experiments was available, NF-YA is closely linked with a cluster containing Group 1 factors, notably FOS, Sp1, Sp2 and CHD2, that in turn have a very high degree of pairwise association and form the strongest cluster (highlighted in red in Figure 3). Notice that for all these factors sequence analysis had indicated the CCAAT box as primary binding motif. A much larger cluster, with less significant correlation with NF-YA, is the one highlighted in green, composed by TFIID (TBP/TAF1), E2F4, ELF1/GABP, MAZ, EGR1, that shares MAX, ETS1, E2F6, PML, KDM5B/PLU1 and Sin3 with Max/MXI1, and at the same time shows a good correlation with the FOS-Sp1-Sp2-CHD2 cluster as well. Other relevant clusters are those formed by GTF2B/GTF2F, ATF3/USF1/USF2 and the one formed by Znf143 and Six5 (yellow box in the heatmap).

In GM12878, NF-YA is once again strongly associated with a FOS-Sp1-CHD2 cluster (red), as in K562, in this case joined also by PBX3 and RFX5, all Group 1 TFs. Note that data for Sp2 were not available in this cell line. Group 1 Six5/Znf143 also show the strong correlation found in K562. A large group with ELF1/ELK1, E-box TFs, PML, SIN3A and TBP is also observable, forming a cluster overlapping with the one identified in K562 (green color) with also a good correlation with CHD2, Sp1 and RFX5. It is

also possible to single out two additional clusters, both visible in HeLa as well, formed by JunD plus C/EBP $\beta$  and BRCA1 plus CoREST, with a low co-association with NF-YA reflecting the results obtained by the sequence analysis for which the enrichment of CCAAT box motifs was lower.

In HeLa cells, where less data sets were available for this analysis, there is again a cluster where FOS is joined by another Group 1 TF, IRF3, but a weaker association with NF-YA and other clusters formed by the E2F family members, by ELK1/4, and the larger subgroup comprising E-box TFs, GTFs, CHD2, MAZ, RFX5, BRCA1 and CoREST. Although ending up clustered elsewhere, Group 1 CHD2 and RFX5 keep however some correlation with the FOS/IRF3 pair. This could also be the effect of the lower co-association for both with NF-YA and NF-YB in this cell line, and also of the lower number of experiments available, that makes the computation of correlations used in clustering to be based on less complete data. In summary, Group 1 TFs tend not only to connect to NF-Y singularly, but also to be clustered together binding the same regions and forming a single regulatory module, further supporting the classification made above, with some notable cell-type specific preferences.

### DNA organization of binding sites

In regions bound both by NF-Y and by another TF, we computed at the single base pair level the distribution of the distance between the respective binding sites, including the possible presence of more than one CCAAT box motif within the same region. This was done only with Group 1 and 2 factors, because of the lack of CCAAT enrichment in Group 3. A positive control was the preferential E-box (CACGTG)-CCAAT box distance, previously identified by us to be 10–12 bps (30). PscanChIP indeed recovered the same CCAAT-E-box bias within regions shared by NF-Y and USF1/2 and MAX, but not with MYC, nor MXI1. In general, 17 out of the 29 Group 1 and 2 factors showed some significant distance bias, and conserved throughout different cell types (see also column ‘Pos bias’ of Table 1). The detailed results are shown in Figure 4. The origin of the coordinates corresponds to the central ‘A’ of the best instance of the CCAAT box in the regions. We plotted for each TF studied the number of times the leftmost (if downstream) or rightmost (if upstream) nucleotide of the respective binding site motif was found to a given distance from the central ‘A’ of CCAAT. As in previous work (10), the distance was computed with respect to the best occurrence of the motif found with a PscanChIP score greater than 0.8 for all factors except Sp1 and Sp2, which have a less conserved binding site motif and for which the threshold employed was 0.9. We used as threshold 0.85 for both instances of the motif as threshold for the presence of a ‘double’ CCAAT. For each TF other than NF-Y, we employed as motif descriptor the JASPAR database (50) matrix associated with it derived from the respective ChIP-Seq experiments, otherwise the ones derived from large scale experiments, like SELEX that showed the greatest enrichment in the analyzed regions.

It is possible to trace a modest positional preference in many cases, some overlapping the CCAAT box itself, as for C/EBP $\beta$ , MafK, RUNX3 and RFX5. The latter has been



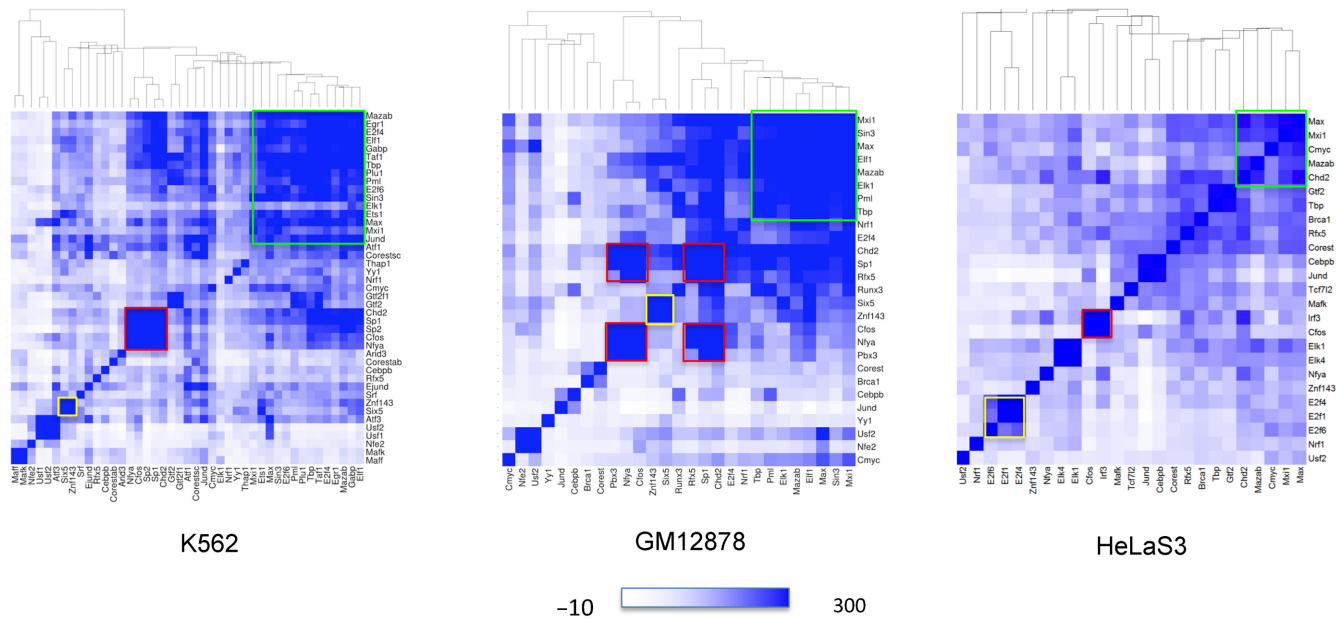


**Figure 3.** Heatmap showing pairwise co-association of TFs within NF-YB bound regions, according to ChIP-Seq peak overlap in the three cell lines studied. Intensity of color in cell  $(x,y)$  is proportional to the co-association score between transcription factors  $x$  and  $y$  within NF-YB peaks, ranging from white (no significant co-association) to darker shades of blue (more significant co-associations). Rows and columns are clustered according to the respective correlations; hence, clustered TFs tend to bind together and have the same global pattern of association with the other TFs within NF-YB bound regions. Colored boxes highlight relevant clusters further discussed in the text.

connected with NF-Y, and a conserved distance of their respective sites has been already shown in the MHC Class II promoters/enhancers (64), it includes a peak at 29 bps with these locations, but it is also present with additional distances. Other TFs show predominant and almost exclusive distance bias, such as E-box binding TFs and Znf143. Six5 shows two sharp peaks, one for an E-box corresponding to the locations of USF1/2, but not MAX, at 12 bps from the CCAAT, and one for Znf143 at 36 bps: indeed, Six5 and Znf143 formed a strong cluster in the co-localization analysis. This configuration is often found in NF-Y-bound repetitive sequences of the LTR12 ERV9 family (26,30).

In the results of this analysis, an interesting feature could be observed with Group 1 factors FOS, IRF3, Sp2 and Sp1, which, as previously discussed, together form the strongest cluster associated with NF-Y and had the CCAAT box as primary sequence motif: the regions they bind together with NF-Y contain a configuration of two CCAAT boxes usually separated by 24–28 and 35–37 bps (Figure 5). The same holds true for PBX3 (for which the CCAAT box was the primary binding site in overlapping regions as well) and RFX5 (in GM12878, given the limited number of overlap regions in K562). Sp1 shows an additional module where the two binding sites are at 19 bps of distance. A closer look at the FOS peaks revealed the additional presence of E-boxes between the two CCAAT, and the complete absence of AP1 motifs as previously mentioned. Factors PBX3, RFX5, Sp2 and Sp1 do show some enrichment of GC-rich Sp1 sites between the two CCAAT boxes, and IRF3 has a combination of E-boxes and Sp1 sites. Overlap with the other EN-CODE ChIP-Seq experiments available revealed that Sp1 and MAX result to be the factors binding these sites located around the double CCAAT area. A similar situation can

be also observed for IRF1 in stimulated K562 cells (data not shown). In general, these double CCAAT sites are enriched in promoters and, for FOS, they are the binding sites for the transcriptionally active AP1-less locations termed ‘proximal-HOT’ devoid of other B-Zip partners (29). We remind that since these analyses were performed on regions resulting to be bound by both NF-Y and each one of the other factors in ChIP-Seq experiments, these multiple CCAAT modules can be reliably considered to be bound by NF-Y *in vivo*.

We also searched for instances of multiple CCAAT boxes in all NF-YB peaks, independently from the presence of additional TFs. Overall, we found that a large number (almost half in K562) of the NF-Y bound regions contained two reliable instances of the motif within 75 bps from the peak summit. The distance plot between those double CCAAT boxes showed, predictably, peaks at 24–27 and 36 bps distance, already found in the locations shown above. That is, about one half of the double CCAAT NF-Y bound regions were in turn associated with regions bound also by one or more of the TFs just discussed. However, two important differences emerged: an additional peak at 43 bps, which is much less evident in regions bound by the FOS/IRF3/Sp2/Sp1/RFX5/PBX3 modules, and a prominent peak at 19 bps, which is completely absent for all these TFs, but Sp1. Further analysis clarified that these latter double CCAAT boxes are mostly present in LTR repetitive sequences of the ERV1 family (29). Thus, essentially three main classes of double CCAAT locations exist: 19 bps apart, mainly located in repetitive sequences; 26 and 36 bps apart, that serve for the FOS/IRF3/Sp1/Sp2/RFX5/PBX3 module, in cooperation with the E-box or GC-rich sites; 43 bps apart,

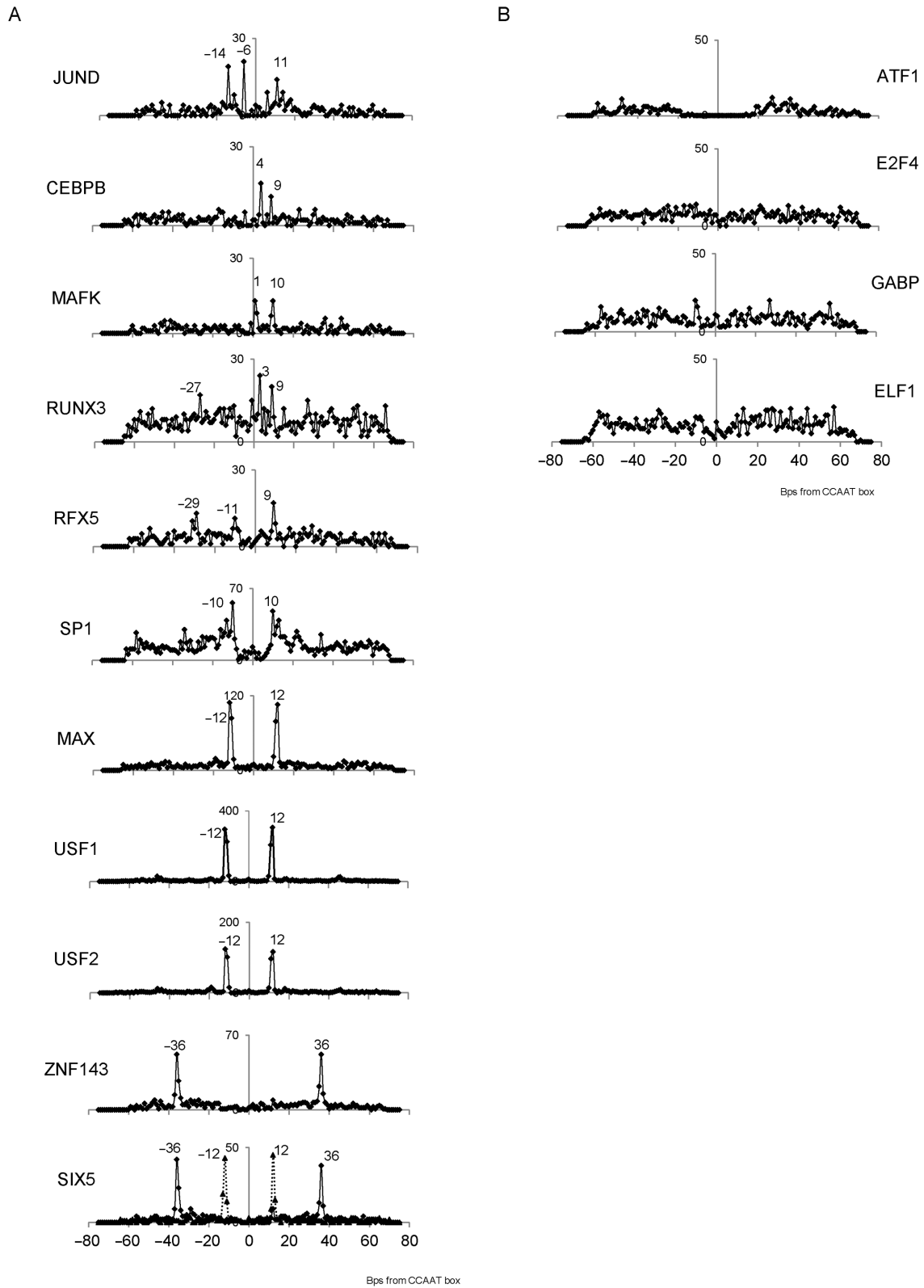


**Figure 4.** Distribution of the distance of binding sites for TFs showing a positional bias with respect to CCAAT boxes in the peak regions bound by both the TF and NF-YB in the K562 cell line (left), and for TFs with CCAAT enrichment but without positional bias (right). The distance is computed from the middle A of CCAAT. For Six5, the full line refers to the Znf143 motif and the dotted line to a E-box.

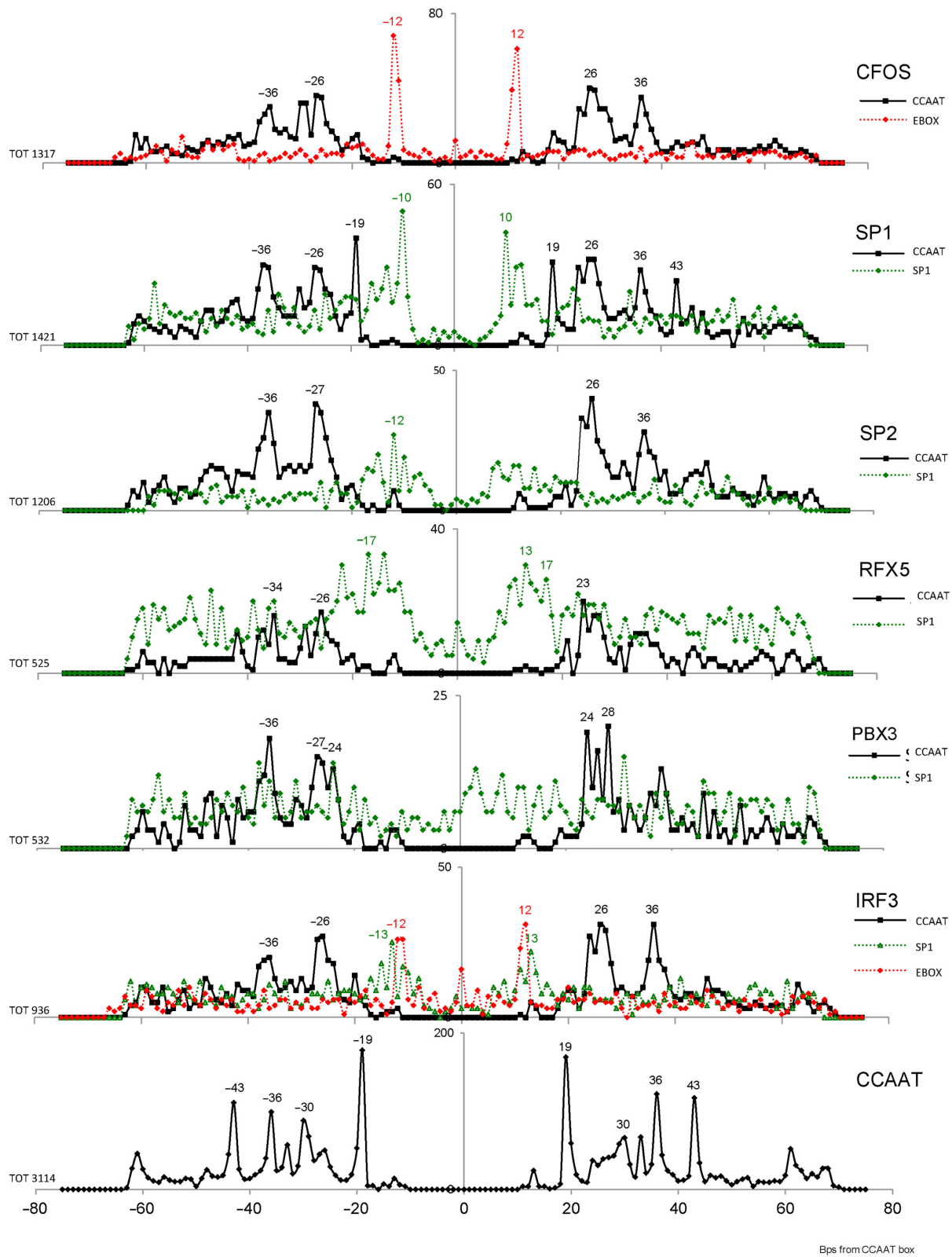


**Figure 5.** Distribution of the distance between two *bona fide* CCAAT boxes for TFs with the CCAAT box as primary binding site, in the peak regions which overlap NF-YB bound regions; the distance is computed from the middle A of CCAAT. Additional enriched motifs with significant positional bias with respect to the CCAAT box are also shown (Sp1 binding site for Sp1, Sp2, RFX5 and IRF3; E-boxes for FOS, IRF3 and PBX3). The analysis was performed for all TFs in the K562 cell line, and in GM12878 for RFX5 and PBX3. The bottom plot shows the overall distance of double CCAAT boxes all in K562 NF-Y-bound regions containing two *bona fide* CCAAT boxes.

for which it remains to be seen which are the TFs—if any—more strongly associated.

### NF-Y requirement for recruitment of E2F4, C/EBP $\beta$ and ELK4

CCAAT-binding by NF-Y has already been shown to be required for the recruitment of numerous TFs and cofactors (33–46). The widespread co-occurrence of NF-Y with other TFs identified here, and the organization of binding sites on DNA, suggests that they are likewise recruited *via* NF-Y. To bring further pieces of evidence for this hypothesis, we inactivated the NF-YB subunit in HeLa cells by shRNA. Then, we studied the binding of three TFs—E2F4, C/EBP $\beta$  and ELK4—one representing each of the Groups, in ChIP assays on a set of genomic locations selected according to the presence of peaks overlapping with NF-YB in ChIP-Seq data (see Materials and Methods). Also, genes encoding for each of the selected TF were monitored to have CCAAT-less promoters. Note that the results could be interpreted either as direct binding of the TFs with NF-Y, or an indirect association via the binding of additional complexes. Specifically, we tested E2F4 because it is one of the few Group 1 TFs without a positional bias of its binding site motif, thus possibly independent from NF-Y binding, and ELK4 as a member of a large family present in all the three Groups, not previously associated to NF-Y activity. The results of qPCRs are shown in Figure 6: we obtained a partial reduction of NF-YB, as assessed by Western blot analysis, whereas the nuclear levels of the three TFs were not changed (Figure 6A); in ChIPs, qPCRs show that the levels of NF-YB binding to CCAAT promoters decreased in NF-YB shRNA-treated cells with respect to scramble shRNA controls. The degree of the decrease matches the levels of NF-YB inactivation. CCAAT-less promoters -ZFPL1, CARS, PALMD, EGR2- were negative for NF-Y binding, as expected (Figure 6B). E2F4 binding followed well the decrease of NF-Y binding, except in the NF-Y-negative ZFPL1 promoter used as control. Group 3 member ELK4 showed a similar behavior on INCENP and PNN, but not on LTN1 and ING1, in which ELK4 binding was unaffected or slightly increased after NF-YB removal. Finally, C/EBP $\beta$  binding was decreased, but we noticed that two control CCAAT-less targets also showed decreased binding, albeit to a lesser degree. Since C/EBP $\beta$  levels are unchanged in NF-YB-inactivated cells, there appears to be some indirect effect, at least partially affecting C/EBP $\beta$  binding.

In summary, in line with the above categorization, these data further support the different degrees of co-association identified by our analysis, indicating that the importance of NF-Y for DNA binding by Group 1 E2F4 is more pervasive than for C/EBP $\beta$  and ELK4.

### Protein–protein interactions

The presence of co-binding with precise spatial arrangements of different TFBSs is an indicator that the respective TFs might directly contact each other, in turn a possible requirement for synergistic transcriptional regulation. We surveyed the BIOGRID repository of published protein–

protein interactions, and added curated data from the literature of NF-Y interactors (see Materials and Methods): 17 proteins, or subunits of complexes, interacting with NF-Y are among the factors studied in this work. Of the 48 factors with significant genome-wide peak overlap with NF-YB according to our criterion, 11 are reported as direct NF-Y interactors (Supplementary Table S4). For comparison, of the other 106 ENCODE factors only 6—GCN5/KAT2A, p300, c-Jun, GATA2, ATF2 and BCL11A—have been reported to interact. Among NF-Y interactors, C/EBP $\beta$ , FOS, Sp1 and USFs showed positional bias for their sites with respect to the CCAAT box, suggesting that the DNA spacing we detected is indeed associated with direct protein–protein interactions. We also retrieved from BIOGRID all protein–protein interactions among all the 48 factors associated with NF-Y, and constructed a network grid: here, again, we noticed a higher density among factors of Group 1 and with a positional bias with respect to the CCAAT box (Supplementary Figure S1). Although further direct protein–protein interactions studies with the TFs identified here with recombinant proteins are required, these data are in general agreement with the model proposed, and reinforce the idea that co-binding on DNA and specific distance biases of the sites are coupled by direct interactions with specific protein domains in NF-Y-TFs modules.

### Functional analysis of co-localizations

We processed expression profiling data upon NF-YA functional inactivation by shRNA in HeLa-S3 cells (see Materials and Methods) in order to single out genes significantly increasing or decreasing their expression as a consequence. This yielded 1492 down- and 1500 up-regulated genes. Considering proximal core promoters of these genes (–450/+50 from TSS), we derived the lists of differentially expressed genes bound by NF-YB, as well as of those co-bound by NF-YB and each of the TFs correlating with NF-Y in HeLa-S3 cells. We performed a gene-ontology (GO) enrichment analysis on each gene list. The most relevant GO terms for each NF-Y/TF combination are shown in Supplementary Table S5A: this allowed for the selection of the NF-Y/TF combinations bound to core promoters in the three cell lines with clear enrichment of selected GO terms (Supplementary Table S5B).

We then categorized the data as a function of NF-Y-dependence. Figure 7 shows, for each enriched GO category, genes belonging to the category split between NF-Y up- and down-regulated, as well as which TFs are significantly associated with NF-Y on the promoters of the genes in the category. Up-regulated genes are those found repressed upon NF-Y inactivation, and vice versa for down-regulated ones. The complete set of genes selected is shown in Supplementary Table S6. It is evident that G2/M genes—annotations *mitotic cell cycle*, *spindle*, *M phase*—as well as *DNA replication* are mostly positively affected by NF-Y and the E2F1/4 module. Vice versa, in NF-Y repressed categories—*nucleosome*, *protein DNA complex*, *chromatin organization*, *ZNF genes*—only E2F4 is present: this fits with the dual role of E2F4 as an activator and repressor, and the activating role of E2F1. We

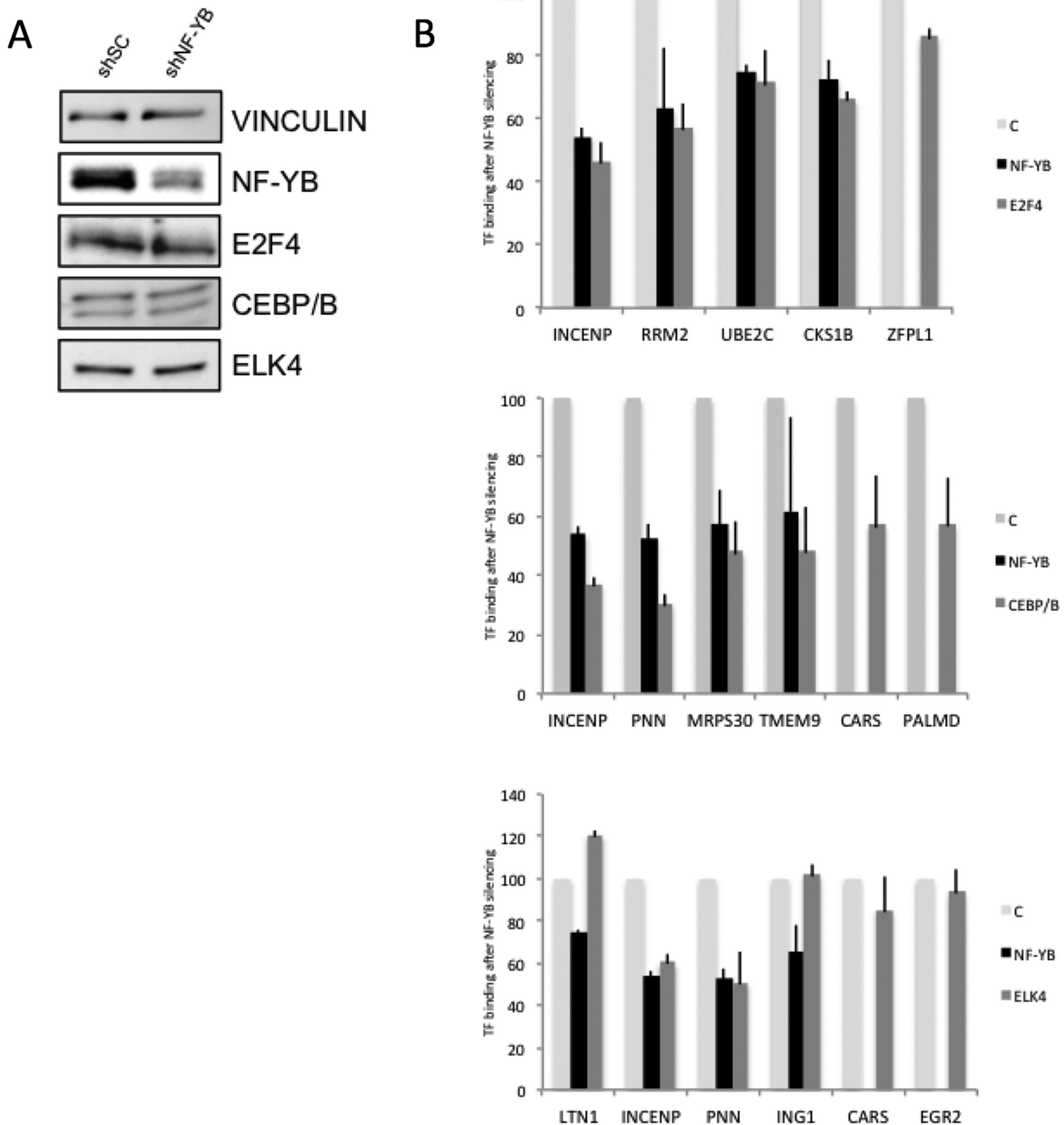


**Figure 6.** Requirement of NF-Y for promoter recruitment of E2F4, C/EBPb and ELK4. (A) Western blot of nuclear extracts of HeLa cells infected with control scramble and NF-YB shRNA with the indicated antibodies. (B) qPCR analysis of ChIP experiments performed on HeLa cells treated as in A, over two biological replicates. The CCAAT and CCAAT-less core promoters regions bound by E2F4, C/EBPb and ELK4 according to ChIP-Seq data are amplified, and the enrichment of NF-YB, E2F4 (Upper), C/EBPb (Middle) and ELK4 (Lower) measured. Binding of both NF-YB and each of the TFs in NF-YB inactivated cells is compared to the respective binding in control HeLa cells (C), which is set at 100 for both.

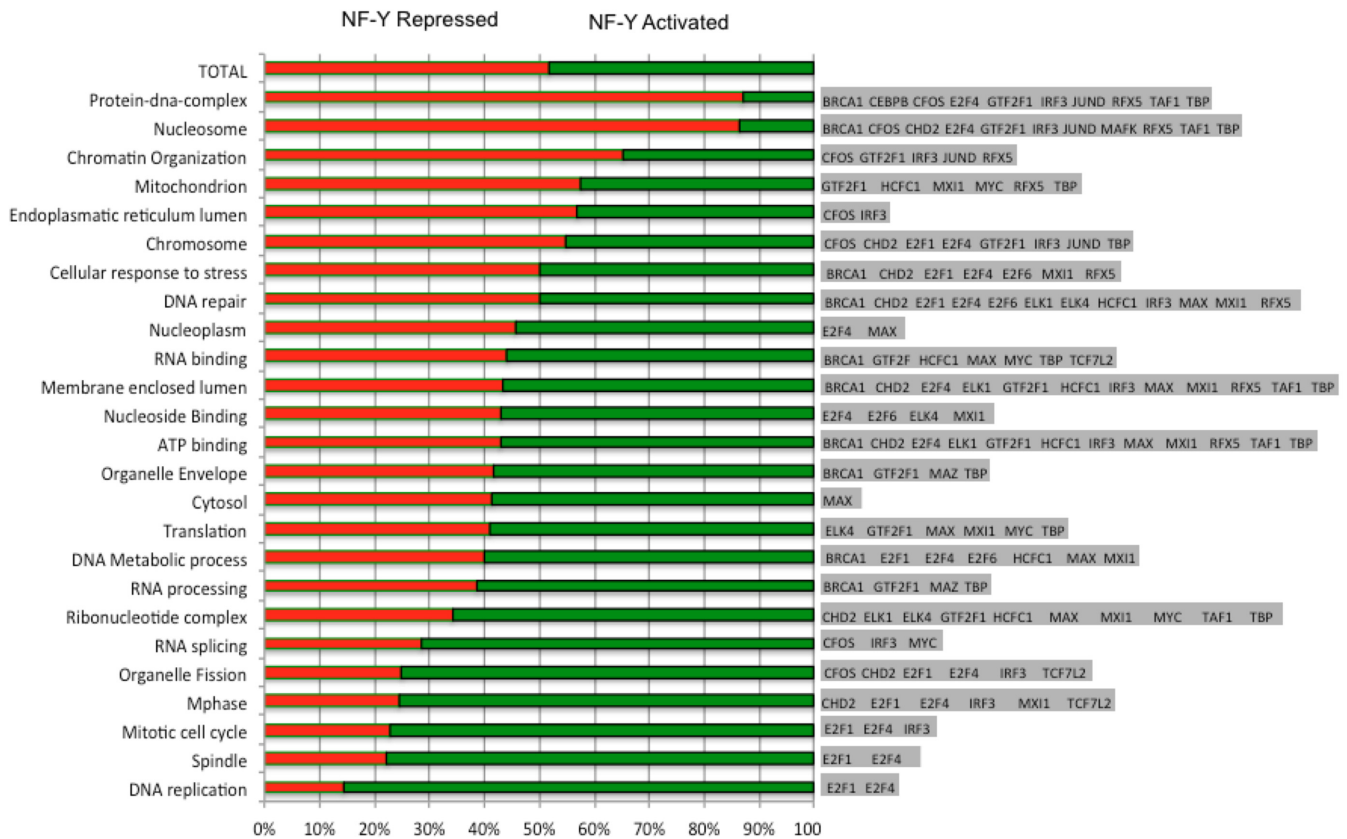


**Figure 7.** Dependence on NF-Y of genes with promoters bound by NF-Y and other TFs, grouped according to GO categories. Left: GO categories found to be enriched in genes bound by NF-Y in combination with the other TFs in the promoter of HeLa cells (the whole data set is available as Supplementary Table S6). Middle: proportion of genes induced or repressed by NF-Y (induced: showing repression upon NF-Y inactivation; vice versa repressed) in each group. Right: TFs enriched together with NF-Y in the promoters of each group.

find B-Zip TFs JunD, MafK and C/EBP $\beta$  mostly on NF-Y repressed genes. RFX5 is also present, but its distribution is more widespread. E-box TFs show little polarization with respect to NF-Y function, with the exception of MYC, which is skewed toward activated categories and on RNA metabolism terms, with the exception of *mitochondrion*. ETS TFs are found on activated categories *ATP* and *nucleoside binding*, *ribonucleotide complex* and *translation*. As for cofactors, CHD2 is widespread, whereas BRCA1 is absent in the NF-Y activated categories, and present in terms related to nuclear transactions (*DNA* and *RNA metabolism*).

## DISCUSSION

We analyzed in detail the correlations of NF-Y with the complete set of available ENCODE data, yielding 48 proteins whose binding showed a substantial link to NF-Y, supported both by sequence analysis and peak overlap. A further classification of factors supported by co-association clusters, *in vivo* ChIP experiments after NF-YB inactivation and protein-protein interaction data, yielded three Groups, which are further discussed.

### Group 1

Sequence-specific TFs represent the majority of factors present in Group 1. Results include previously reported ob-

servations on co-associations with E-box binding TFs (30), extended to other cell lines. More importantly, several novel associations were brought into light. Sp1 peaks do show a canonical binding site at a preferential distance of 10 bps 5' and 3' of a CCAAT box, a distance in line with a general sequence analysis of CCAAT promoters (10), and within the range of the extensive DNA contacts (25/28 bps) made by the HFD subunits of the NF-Y trimer. ChIP-Seq in mouse MEFs and HEK293 cells showed a significant enrichment of CCAAT boxes in Sp2 peaks (47,61), which is thus confirmed by our analysis. Using the elegant system of mouse Sp2 KO ES cells overexpressing different Sp2 mutants, it has been demonstrated that the Q-rich activation domain of Sp2, not the Zn finger DNA-binding domain, is required for NF-Y-mediated recruitment to CCAAT promoters (47). NF-Y and Sp1 interact directly (65–67) and the parts mediating binding are indeed Sp1-B and NF-YA/NF-YC Q-rich activation domains: intriguingly, these domains show a traceable phylogenetic resemblance (68). Both interacting regions of NF-Y undergo alternative splicing (31,69), producing isoforms with different and specific cooperativity with Sp1 family members (70). Our finding that precisely spaced pairs of CCAAT boxes bound by NF-Y are present in Sp2, and to some extent, Sp1 peaks, mostly located within promoters, is a further step in the fine definition of this regulatory module, present in many promoters.

The widespread intersection of FOS with NF-Y sites already reported in K562 (29,30), is confirmed in other cell types. Importantly, we define here the double CCAAT arrangement required in such peaks, which is not found in the peaks of the related FOSL1 and FOSL2, that do not overlap significantly with NF-Y sites. FOS is known to bind as a heterodimer with other members of the B-Zip family to AP1 sites: the lack of AP1 sites in FOS/NF-Y locations indicates that B-Zip partners absent in ENCODE are likely not involved in the interaction. The recruitment of FOS is rather unique among B-Zip proteins, which are mostly found in Group 2 with AP1 sites, and it could be due to protein-protein interactions with NF-Y (29). It is possible that, as for Sp2, activation domains, instead of DNA-binding domains might be involved.

RFX5 is a member of the RFX family binding to the X box, an element originally discovered in MHC Class II genes, along with the Y box (64). The MHC Class II X box is recognized by RFX5, RFX-ANK and RFXAP (71). NF-Y cooperates with RFX5 (55,72), with direct protein-protein interactions (55,56). The relative distance is conserved and functionally essential, and this configuration is inactive without the tissue-specific co-activator CIITA. The X box motif is indeed present in RFX5 peaks (27), but the (double) CCAAT box is highlighted as the primary binding site in our analysis when RFX5 co-localizes with NF-Y. Thus, the RFX5/NF-Y partnership, shown to be functional in highly specific gene sets, is more generally widespread and their overlap is second only to FOS. Surprisingly, the role of NF-Y in such units is not invariably associated to genes whose expression decreases after NF-YA inactivation, as in the case of MHC Class II.

Two more TFs associated to the double CCAAT box motif are IRF3 and PBX3. IRF3 is involved in transcriptional regulation of immune response genes (73), and it is devoid of the expected IRF binding motif (28). The double CCAAT motif can also be observed in stimulated K562 cells data of the related IRF1 (data not shown). IRF3 is present both in the most activated (*mitosis, organelle fixation*) and repressed (*nucleosome, protein DNA complex, ER lumen*) functional categories associated with NF-Y, suggesting that it might positively or negatively impact on NF-Y function. PBX3 is a TALE homeodomain TF expressed during development, which controls patterning and differentiation. Recently, PBX3 expression was linked to the development of acute myeloid leukemias (AML), in conjunction with specific HOXAs. CCAAT boxes were also found enriched in the peaks of PBX1, a TF similar to PBX3, when associated with Prep1 (74): hence, this link might hold true also for other family members. Analysis of ENCODE data detected NF-Y binding sites in regions bound by Sp1 and PBX3 (75).

The analysis of ENCODE data has generalized the concept that some TFs are tethered to DNA *via* association with other TFs, in addition to their own target (26,28). We found here that the double precisely spaced CCAAT module is the landing platform of Group 1 TFs FOS, Sp2, Sp1, RFX5, PBX3 and IRF3, when these TFs bind DNA together with NF-Y. In general, these data support the presence of specific multi-protein complexes associated with the multi-CCAAT platform. Promoters of cell cycle regulated genes with multiple CCAAT boxes were originally de-

scribed as repressed upon wild-type p53 activation—and vice versa activated by mutp53—in the apparent absence of p53REs (76). The 26–30 bps distance found here corresponds to such promoters, many of which are of cell-cycle genes, and it is specifically predominant, together with the 36 bps distance. TFs found to recognize this NF-Y platform share with p53, and family members, the capacity to influence growth decisions. While Sp1, Sp2 and RFX5 peaks are found with some Sp1 motifs between the two CCAAT, FOS and PBX3 have an enrichment of E-boxes, IRF3 a combination of both TFBSs: this shows that each TF has additional specific requirements within these modules. The 19 bps distance is only found in LTR sequences. Note the complete absence of double CCAAT boxes closer than 19 bps, which fits perfectly with the minimal distance requirement for double NF-Y binding, originally determined by *in vitro* experiments (77), and recently rationalized by the 3D NF-Y/CCAAT structure (17).

All E2Fs family members analyzed by ENCODE are correlated with NF-Y, not only in cell cycle regulated genes, but also in genes with different functional annotations. E2F4, shows the strongest link, and the requirement of NF-Y for efficient promoter association (Figure 6). The NF-Y-E2F4 partnership is complex and associated with different functional outcomes: repression in *nucleosome* and *protein DNA complex* genes, activation in *DNA replication* and *mitosis* genes. We find a limited enrichment for the canonical E2F binding sites in E2F1/4/6 sites, in accordance to previous reports (62,78). Several non-mutually exclusive explanations were brought forward: E2Fs could be recruited *via* indirect tethering by unrelated TFs, such as NF-Y and E-box binding TFs. E2Fs could bind *in vivo* to variations of the *in vitro* characterized motif; a third possibility is that E2Fs are part of larger complexes, with different DNA-binding specificity. The case of E2F4 binding to G2/M promoters is likely explicative: they work through multiple evolutionarily conserved CCAAT and CDE-CHR elements, which are controlled by the DREAM complex, of which E2F4 is a subunit (79). Since the DREAM subunits B-MYB, Lin-9, and Lin-54 bind DNA, it is likely that the specificity of E2F4 is modified by these subunits. Thus, the lack of preferential distances between CCAAT boxes and E2F sites should be re-evaluated once the variety of E2F motifs are dissected, and genomic locations of DREAM subunits are collected. A step in this direction was the reported enrichment of CCAAT boxes in the locations bound by FOXM1, a protein that helps DREAM activity (80).

## Group 2

In Group 2 the most abundant class of factors are B-Zip TFs: (i) JunD, MafF/K band ATF1/3 which have AP1, CRE or related sequences in the majority of their peaks. (ii) C/EBPb, whose robust overlap with NF-Y was somewhat expected, since several promoters are already known to be co-activated by NF-Y and C/EBPs (81–83). NF-Y was shown to directly interact with several B-Zip TFs like ATF3 (54), c-Jun (84) and ATF2/6 (67,85–88).

A novel class connected with NF-Y is ETS domain proteins, which all recognize a similar, albeit not identical motif (89). All members of this class analyzed by ENCODE

(GABP, ELK1, ELF1, ELK4, ETS1, SRF) are present in our list; only some (ELF1, GABP, SRF) show enrichment for CCAAT boxes in their peaks. There are two common features in this family: the first is that none is ubiquitously present: ELF1 is present in 3 of 4 cell lines, GABPA in 1 of 6, ELK4 in 3 of 7, ELK1 and ETS1 in 2 of 3. In most cell lines, there is one or more ETS TF associated with NF-Y, but never all of them. The second is that their binding motif shows no distance bias with respect to the CCAAT box, and indeed their binding appear to be relatively independent from NF-Y, in the ChIP experiments of Figure 6. They are co-associated in functional categories of cytoplasmic transactions, with the exception of *DNA repair*, in promoters well balanced between NF-Y activation and repression. Interestingly, dissection of the genomic ERK2 pathway in hESCs identified pivotal ELK1 sites, further validated by ChIP-Seq experiments, as well as CCAAT boxes and Sp1, E2F, NRF1 TFBSs (90). Thus, this set of TFs might be particularly relevant in signaling pathways.

The NF-Y link to the zinc finger protein Znf143 is novel and potentially important, as they are both clearly essential for Six5 binding (note their tight clustering in K562 and GM12878 cells shown in Figure 3) with a very precise spacing; the composite sites often include E-boxes in intervening positions. Many of these sites are in repetitive sequences of the LTR ERV9 subfamilies. Interestingly, both MAZ and SIX family members, including Six5, are involved in the differentiation of muscle cells (91,92).

As for cofactors, BRCA1, which is often associated with CoREST and RFX5 in HeLa-S3 data, was implicated in the transcriptional regulation of the GADD45 promoter, notably through the interplay between CCAAT/NF-Y and OCTA/POU2F (93). The NF-Y association in HeLa-S3 is in genes involved in nuclear and cytoplasmic transactions, often with PML (*RNA-binding*, *ATP binding*, *nucleosome* and *DNA-binding complex*), in which NF-Y is generally repressive. BRCA1 is involved in DNA replication and recombination, KDM5B in DNA-repair and indeed required for recruitment of BRCA1 at sites of homologous recombination (94); these links might hint at a possible role of NF-Y in DNA metabolisms other than transcription, an aspect poorly investigated so far, but certainly worth to be explored in the future.

### Group 3

GTFs are prominent in this group. They are known to bind near TSSs, and their overlap with NF-Y regions was somewhat expected, given NF-Y typical promoter location at  $-60/-100$  from TSSs. The co-associations of TATA-binding TBP, of the TFIID subunit TAF1 ( $>60\%$  of overlap in the three cell lines) and of GTF2B (TFIIB), known to associate to TBP/TATA complexes, resulted in fact to be significant. Note that TBP, the one GTF with clear sequence-specificity, is in Group 1. NF-Y physical interactions with several subunits of TFIID were reported (95), although TAF1 was not tested. In most of these NF-Y/GTFs clusters, RNA Pol II is also present ( $>70\%$ ) and the genes are transcriptionally active. Indeed, NF-Y binding sites were among the most enriched ones in RNA Pol II peaks in PscanChIP analysis of 17 out of the 21 ENCODE Pol II

data sets (Not shown). In addition, the RNA Pol II associated GTF2F1 (TFIIF) is also well correlated to NF-Y peaks. Note that ChIP experiments after NF-Y removal supported a role of NF-Y in RNA Pol II recruitment to ER-stress promoters (96), suggesting that it is important for the landing of at least some components of the GTF machinery on the core promoter, prior to induction of RNA synthesis.

NRF1 is a b-Zip CNC (Cap-'n'-Collar) TF important for the activation of genes involved in mitochondrial pathways (97): in ENCODE data, the two binding motifs overlapped significantly in the respective ChIP-Seqs (see also Supplementary Figure S8 (26)), while a study in MCF7 cells showed a lack of CCAAT boxes in NRF1 controlled genes, as well as non overlapping cofactors dependence (8). Our analyses agree upon the modest co-occurrence of NF-Y motifs in NRF1 sites, but we do detect a significant co-occurrence of peaks: we tend to interpret these results as a sign that the two TFs co-regulate selected groups of promoters, among which G2/M genes (8,98).

Of the more than 30 transcriptional co-factors analyzed so far by the ENCODE project, only a few are significantly associated to NF-Y, including the four proteins involved in the regulation of methylations of histone H3K4, major epigenetic marks positioned on open chromatin. Plu1/KDM5B, a demethylase of H3K4me3, is in Group 3. It was shown to be associated to promoters and enhancers of ES cells TFs, notably SOX2, OCT4 and Nanog (99), to prevent spreading of H3K4 methylations to the body of the gene. Given the co-association of NF-Y with such ESCs TFs (34), it is reasonable to suggest a link with KDM5B in such cells as well. The other H3K4me3 regulators are in Group 1 (HCFC1 and CHD2) and Group 2 (CoREST). HCFC1, originally identified as a co-activator of viral proteins, interacts with MLL complexes, the 'writers' of these marks (90); E2Fs activity is dependent upon HCFC1, notably in cell-cycle promoters (100,101). HCFC1 peaks were shown to be enriched in Znf143, Thap11, YY1 and GABP motifs (93), and indeed we find here that Znf143, GABP, YY1 and NF-Y peaks significantly overlap. CoREST recognizes nucleosomes through the SWR domain (102) and is part of repressive complexes that demethylate H3K4me2, although it is also associated with androgen-dependent activated genes (103). Finally, CHD2 is a member of a large family of helicases involved in chromatin remodeling; the highly related CHD1 is known to be a 'reader' of the H3K4me3 mark (104,105): the overlap with NF-Y is only observed for CHD2, indicating some specificity in the interplay. The strong correlations of NF-Y with epigenetic marks were reported earlier, in genomic studies (29,30,32) and in cause/effect experiments upon NF-Y inactivation (17,38,71). Overall, the data reinforce the role of NF-Y in recruiting proteins that control—positively and negatively—H3K4 methylations.

The conclusions reached in this study will impact the biochemical characterization of NF-Y/TFs interplay on DNA: our recent description of the three dimensional structure of NF-Y bound to a single CCAAT box will be extended to include the double CCAAT platform, according to the rules established here. In addition, the availability of 3D structures of NF-Y, as well as of some of the identified HLH, B-Zip, HD and ZNF TFs, with the respective DNA sites, will



allow molecular modeling of the interplays and the reconstruction of interactions by structural biology approaches, according to priorities derived by the categorization described here.

## SUPPLEMENTARY DATA

Supplementary Data are available at NAR Online.

## FUNDING

Funding for open access charge: Italian Consiglio Nazionale delle Ricerche (CNR) flagship project 'EPIGEN' (to G.P.); AIRC [14130 to R.M.].

*Conflict of interest statement.* None declared.

## REFERENCES

- Suzuki, Y., Yamashita, R., Shiota, M., Sakakibara, Y., Chiba, J., Mizushima-Sugano, J., Nakai, K. and Sugano, S. (2004) Sequence comparison of human and mouse genes reveals a homologous block structure in the promoter regions. *Genome Res.*, **14**, 1711–1718.
- Fitzgerald, P.C., Shlyakhtenko, A., Mir, A.A. and Vinson, C. (2004) Clustering of DNA sequences in human promoters. *Genome Res.*, **14**, 1562–1574.
- Xie, X., Lu, J., Kulbokas, E.J., Golub, T.R., Mootha, V., Lindblad-Toh, K., Lander, E.S. and Kellis, M. (2005) Systematic discovery of regulatory motifs in human promoters and 3' UTRs by comparison of several mammals. *Nature*, **434**, 338–345.
- Häkkinen, A., Healy, S., Jacobs, H.T. and Ribeiro, A.S. (2011) Genome wide study of NF-Y type CCAAT boxes in unidirectional and bidirectional promoters in human and mouse. *J. Theor. Biol.*, **281**, 74–83.
- Lin, J.M., Collins, P.J., Trinklein, N.D., Fu, Y., Xi, H., Myers, R.M. and Weng, Z. (2007) Transcription factor binding and modified histones in human bidirectional promoters. *Genome Res.*, **17**, 818–827.
- Vardhanabhuti, S., Wang, J. and Hannehalli, S. (2007) Position and distance specificity are important determinants of cis-regulatory motifs in addition to evolutionary conservation. *Nucleic Acids Res.*, **35**, 3203–3213.
- Yokoyama, K.D., Ohler, U. and Wray, G.A. (2009) Measuring spatial preferences at fine-scale resolution identifies known and novel cis-regulatory element candidates and functional motif-pair relationships. *Nucleic Acids Res.*, **37**, e92.
- Benner, C., Konovalov, S., Mackintosh, C., Hutt, K.R., Stunnenberg, R. and Garcia-Bassets, I. (2013) Decoding a signature-based model of transcription cofactor recruitment dictated by cardinal cis-regulatory elements in proximal promoter regions. *PLoS Genet.*, **9**, e1003906.
- Stergachis, A.B., Neph, S., Sandstrom, R., Haugen, E., Reynolds, A.P., Zhang, M., Byron, R., Canfield, T., Stelting-Sun, S., Lee, K. *et al.* (2014) Conservation of trans-acting circuitry during mammalian regulatory evolution. *Nature*, **515**, 365–370.
- Dolfini, D., Zambelli, F., Pavesi, G. and Mantovani, R. (2009) A perspective of promoter architecture from the CCAAT box. *Cell Cycle*, **8**, 4127–4137.
- Rhodes, D.R., Kalyana-Sundaram, S., Mahavisno, V., Barrette, T.R., Ghosh, D. and Chinnaiyan, A.M. (2005) Mining for regulatory programs in the cancer transcriptome. *Nat. Genet.*, **37**, 579–583.
- Sinha, S., Adler, A.S., Field, Y., Chang, H.Y. and Segal, E. (2008) Systematic functional characterization of cis-regulatory motifs in human core promoters. *Genome Res.*, **18**, 477–488.
- Goodarzi, H., Elemento, O. and Tavazoie, S. (2009) Revealing global regulatory perturbations across human cancers. *Mol. Cell*, **36**, 900–911.
- Balwierz, P.J., Pachkov, M., Arnold, P., Gruber, A.J., Zavolan, M. and van Nimwegen, E. (2014) ISMARA: automated modeling of genomic signals as a democracy of regulatory motifs. *Genome Res.*, **24**, 869–884.
- Dolfini, D. and Mantovani, R. (2013) Targeting the Y/CCAAT box in cancer: YB-1 (YBX1) or NF-Y? *Cell Death Differ.*, **20**, 676–685.
- Huber, E.M., Scharf, D.H., Hortschansky, P., Groll, M. and Brakhage, A.A. (2012) DNA minor groove sensing and widening by the CCAAT-binding complex. *Structure*, **20**, 1757–1768.
- Nardini, M., Gnesutta, N., Donati, G., Gatta, R., Forni, C., Fossati, A., Vonrhein, C., Moras, D., Romier, C., Bolognesi, M. *et al.* (2013) Sequence-specific transcription factor NF-Y displays histone-like DNA binding and H2B-like ubiquitination. *Cell*, **152**, 132–143.
- Bhattacharya, A., Deng, J.M., Zhang, Z., Behringer, R., de Crombrughe, B. and Maity, S.N. (2003) The B subunit of the CCAAT box binding transcription factor complex (CBF/NF-Y) is essential for early mouse development and cell proliferation. *Cancer Res.*, **63**, 8167–8172.
- Luo, R., Klumpp, S.A., Finegold, M.J. and Maity, S.N. (2011) Inactivation of CBF/NF-Y in postnatal liver causes hepatocellular degeneration, lipid deposition, and endoplasmic reticulum stress. *Sci. Rep.*, **1**, 136.
- Bungartz, G., Land, H., Scadden, D.T. and Emerson, S.G. (2012) NF-Y is necessary for hematopoietic stem cell proliferation and survival. *Blood*, **119**, 1380–1389.
- Yamanaka, T., Tosaki, A., Kurosawa, M., Matsumoto, G., Koike, M., Uchiyama, Y., Maity, S.N., Shimogori, T., Hattori, N. and Nukina, N. (2014) NF-Y inactivation causes atypical neurodegeneration characterized by ubiquitin and p62 accumulation and endoplasmic reticulum disorganization. *Nat. Commun.*, **5**, 3354.
- Lu, Y.H., Dallner, O.S., Birsoy, K., Fayzikhodjaeva, G. and Friedman, J.M. (2015) Nuclear Factor-Y is an adipogenic factor that regulates leptin gene expression. *Mol. Metab.*, **4**, 392–405.
- Dolfini, D., Gatta, R. and Mantovani, R. (2012) NF-Y and the transcriptional activation of CCAAT promoters. *Crit. Rev. Biochem. Mol. Biol.*, **47**, 29–49.
- ENCODE Project Consortium. (2012) An integrated encyclopedia of DNA elements in the human genome. *Nature*, **489**, 57–74.
- Gerstein, M.B., Kundaje, A., Hariharan, M., Landt, S.G., Yan, K.K., Cheng, C., Mu, X.J., Khurana, E., Rozowsky, J., Alexander, R. *et al.* (2012) Architecture of the human regulatory network derived from ENCODE data. *Nature*, **489**, 91–100.
- Wang, J., Zhuang, J., Iyer, S., Lin, X., Whitfield, T.W., Greven, M.C., Pierce, B.G., Dong, X., Kundaje, A., Cheng, Y. *et al.* (2012) Sequence features and chromatin structure around the genomic regions bound by 119 human transcription factors. *Genome Res.*, **22**, 1798–1812.
- Wang, J., Zhuang, J., Iyer, S., Lin, X.Y., Greven, M.C., Kim, B.H., Moore, J., Pierce, B.G., Dong, X., Virgil, D. *et al.* (2013) Factorbook.org: a Wiki-based database for transcription factor-binding data generated by the ENCODE consortium. *Nucleic Acids Res.*, **41**, D171–D176.
- Kheradpour, P. and Kellis, M. (2014) Systematic discovery and characterization of regulatory motifs in ENCODE TF binding experiments. *Nucleic Acids Res.*, **42**, 2976–2987.
- Xie, D., Boyle, A.P., Wu, L., Zhai, J., Kawli, T. and Snyder, M. (2013) Dynamic trans-acting factor colocalization in human cells. *Cell*, **155**, 713–724.
- Fleming, J.D., Pavesi, G., Benatti, P., Imbriano, C., Mantovani, R. and Struhl, K. (2013) NF-Y coassociates with FOS at promoters, enhancers, repetitive elements, and inactive chromatin regions, and is stereo-positioned with growth-controlling transcription factors. *Genome Res.*, **23**, 1195–1209.
- Testa, A., Donati, G., Yan, P., Romani, F., Huang, T.H., Viganò, M.A. and Mantovani, R. (2005) Chromatin immunoprecipitation (ChIP) on chip experiments uncover a widespread distribution of NF-Y binding CCAAT sites outside of core promoters. *J. Biol. Chem.*, **280**, 13606–13615.
- Ceribelli, M., Dolfini, D., Merico, D., Gatta, R., Viganò, A.M., Pavesi, G. and Mantovani, R. (2008) The histone-like NF-Y is a bifunctional transcription factor. *Mol. Cell Biol.*, **28**, 2047–2058.
- Sherwood, R.I., Hashimoto, T., O'Donnell, C.W., Lewis, S., Barkal, A.A., van Hoff, J.P., Karun, V., Jaakkola, T. and Gifford, D.K. (2014) Discovery of directional and nondirectional pioneer transcription factors by modeling DNase profile magnitude and shape. *Nat. Biotechnol.*, **32**, 171–178.
- Oldfield, A.J., Yang, P., Conway, A.E., Cinghu, S., Freudenberg, J.M., Yellaboina, S. and Jothi, R. (2014) Histone-fold domain protein NF-Y promotes chromatin accessibility for cell type-specific master transcription factors. *Mol. Cell*, **55**, 708–722.

35. Dolfini, D., Minuzzo, M., Pavesi, G. and Mantovani, R. (2012) The short isoform of NF-YA belongs to the embryonic stem cell transcription factor circuitry. *Stem Cells*, **30**, 2450–2459.
36. Kabe, Y., Yamada, J., Uga, H., Yamaguchi, Y., Wada, T. and Handa, H. (2005) NF-Y is essential for the recruitment of RNA polymerase II and inducible transcription of several CCAAT box-containing genes. *Mol. Cell. Biol.*, **25**, 512–522.
37. Yu, F.X. and Luo, Y. (2009) Tandem ChoRE and CCAAT motifs and associated factors regulate Txnip expression in response to glucose or adenosine-containing molecules. *PLoS One*, **4**, e8397.
38. Fossati, A., Dolfini, D., Donati, G. and Mantovani, R. (2011) NF-Y recruits Ash2L to impart H3K4 trimethylation on CCAAT promoters. *PLoS One*, **6**, e17220.
39. Lin, Y.C., Chen, Y.N., Lin, K.F., Wang, F.F., Chou, T.Y. and Chen, M.Y. (2014) Association of p21 with NF-YA suppresses the expression of Polo-like kinase 1 and prevents mitotic death in response to DNA damage. *Cell Death Dis.*, **5**, e987.
40. Tiwari, V.K., Stadler, M.B., Wirbelauer, C., Paro, R., Schübeler, D. and Beisel, C. (2011) A chromatin-modifying function of JNK during stem cell differentiation. *Nat. Genet.*, **44**, 94–100.
41. Di Agostino, S., Strano, S., Emiliozzi, V., Zerbini, V., Mottolose, M., Sacchi, A., Blandino, G. and Piaggio, G. (2006) Gain of function of mutant p53: the mutant p53/NF-Y protein complex reveals an aberrant transcriptional mechanism of cell cycle regulation. *Cancer Cell*, **10**, 191–202.
42. Weissmueller, S., Machado, E., Saborowski, M., Morris, J.P. 4th, Wagenblast, E., Davis, C.A., Moon, S.H., Pfister, N.T., Tschaharganeh, D.F., Kitzing, T. et al. (2014) Mutant p53 drives pancreatic cancer metastasis through cell-autonomous PDGF receptor SH. *Pfister*. *Cell*, **157**, 382–394.
43. Luo, R., Lu, J.F., Hu, Q. and Maity, S.N. (2008) CBF/NF-Y controls endoplasmic reticulum stress induced transcription through recruitment of both ATF6(N) and TBP. *J. Cell. Biochem.*, **104**, 1708–1723.
44. Huang, X., Zhang, Y., Tang, Y., Butler, N., Kim, J., Guessous, F., Schiff, D., Mandell, J. and Abounader, R. (2013) A novel PTEN/mutant p53/c-Myc/Bcl-XL axis mediates context-dependent oncogenic effects of PTEN with implications for cancer prognosis and therapy. *Neoplasia*, **15**, 952–965.
45. Arampatzis, P., Gialitakis, M., Makatounakis, T. and Papamatheakis, J. (2013) Gene-specific factors determine mitotic expression and bookmarking via alternate regulatory elements. *Nucleic Acids Res.*, **41**, 2202–2215.
46. Shi, Z., Chiang, C.I., Labhart, P., Zhao, Y., Yang, J., Mistretta, T.A., Henning, S.J., Maity, S.N. and Mori-Akiyama, Y. (2015) Context-specific role of SOX9 in NF-Y mediated gene regulation in colorectal cancer cells. *Nucleic Acids Res.*, **43**, 6257–6269.
47. Völkel, S., Stielow, B., Finkernagel, F., Stiewe, T., Nist, A. and Suske, G. (2015) Zinc finger independent genome-wide binding of Sp2 potentiates recruitment of histone-fold protein Nf-y distinguishing it from Sp1 and Sp3. *PLoS Genet.*, **11**, e1005102.
48. Rosenbloom, K.R., Armstrong, J., Barber, G.P., Casper, J., Clawson, H., Diekhans, M., Dreszer, T.R., Fujita, P.A., Guruvadoo, L., Haussler, M. et al. (2015) The UCSC Genome Browser database: 2015 update. *Nucleic Acids Res.*, **43**, D670–D681.
49. Zambelli, F., Pesole, G. and Pavesi, G. (2013) PscanChIP: finding over-represented transcription factor-binding site motifs and their correlations in sequences from ChIP-Seq experiments. *Nucleic Acids Res.*, **41**, W535–W543.
50. Mathelier, A., Zhao, X., Zhang, A.W., Parcy, F., Worsley-Hunt, R., Arenillas, D.J., Buchman, S., Chen, C.Y., Chou, A., Ienasescu, H. et al. (2014) JASPAR 2014: an extensively expanded and updated open-access database of transcription factor binding profiles. *Nucleic Acids Res.*, D142–D147.
51. Mantovani, R. (1998) A survey of 178 NF-Y binding CCAAT boxes. *Nucleic Acids Res.*, **26**, 1135–1143.
52. Costessi, A., Mahrouf, N., Tijchon, E., Stunnenberg, R., Stoel, M.A., Jansen, P.W., Sela, D., Martin-Brown, S., Washburn, M.P., Florens, L. et al. (2011) The tumour antigen PRAME is a subunit of a Cul2 ubiquitin ligase and associates with active NFY promoters. *EMBO J.*, **30**, 3786–3798.
53. Stark, C., Breitkreutz, B.J., Reguly, T., Boucher, L., Breitkreutz, A. and Tyers, M. (2006) BioGRID: a general repository for interaction datasets. *Nucleic Acids Res.*, **34**, D535–D539.
54. Lindaman, L.L., Yeh, D.M., Xie, C., Breen, K.M. and Coss, D. (2013) Phosphorylation of ATF2 and interaction with NFY induces c-Jun in the gonadotrope. *Mol. Cell Endocrinol.*, **365**, 316–326.
55. Villard, J., Peretti, M., Masternak, K., Barras, E., Caretti, G., Mantovani, R. and Reith, W. (2000) A functionally essential domain of RFX5 mediates activation of major histocompatibility complex class II promoters by promoting cooperative binding between RFX and NF-Y. *Mol. Cell. Biol.*, **20**, 3364–3376.
56. Jabrane-Ferrat, N., Nekrep, N., Tosi, G., Esserman, L.J. and Peterlin, B.M. (2002) Major histocompatibility complex class II transcriptional platform: assembly of nuclear factor Y and regulatory factor X (RFX) on DNA requires RFX5 dimers. *Mol. Cell. Biol.*, **22**, 5616–5625.
57. Ito, Y., Zhang, Y., Dangaria, S., Luan, X. and Diekwisch, T.G. (2011) NF-Y and USF1 transcription factor binding to CCAAT-box and E-box elements activates the CP27 promoter. *Gene*, **473**, 92–99.
58. Zhu, J., Zhang, Y., Joe, G.J., Pompetti, R. and Emerson, S.G. (2005) NF-Y activates multiple hematopoietic stem cell (HSC) regulatory genes and promotes HSC self-renewal. *Proc. Natl. Acad. Sci. U.S.A.*, **102**, 11728–11733.
59. van Wageningen, S., Breems-de Ridder, M.C., Nigten, J., Nikoloski, G., Erpelinck-Verschueren, C.A., Löwenberg, B., de Witte, T., Tenen, D.G., van der Reijden, B.A. and Jansen, J.H. (2008) Gene transactivation without direct DNA binding defines a novel gain-of-function for PML-RARalpha. *Blood*, **111**, 1634–1643.
60. Tanaka, Y., Nakamura, A., Morioka, M.S., Inoue, S., Tamamori-Adachi, M., Yamada, K., Taketani, K., Kawauchi, J., Tanaka-Okamoto, M., Miyoshi, J. et al. (2011) Systems analysis of ATF3 in stress response and cancer reveals opposing effects on pro-apoptotic genes in p53 pathway. *PLoS One*, **6**, e26848.
61. Terrados, G., Finkernagel, F., Stielow, B., Sadic, D., Neubert, J., Herdt, O., Krause, M., Scharfe, M., Jarek, M. and Suske, G. (2012) Genome-wide localization and expression profiling establish Sp2 as a sequence-specific transcription factor regulating vitally important genes. *Nucleic Acids Res.*, **40**, 7844–7857.
62. Lee, B.K., Bhinge, A.A. and Iyer, V.R. (2011) Wide-ranging functions of E2F4 in transcriptional activation and repression revealed by genome-wide analysis. *Nucleic Acids Res.*, **39**, 3558–3573.
63. Barberis, A., Superti-Furga, G. and Busslinger, M. (1987) Mutually exclusive interaction of the CCAAT-binding factor and of a displacement protein with overlapping sequences of a histone gene promoter. *Cell*, **50**, 347–359.
64. Benoist, C. and Mathis, D. (1990) Regulation of major histocompatibility complex class-II genes: X, Y and other letters of the alphabet. *Annu. Rev. Immunol.*, **8**, 681–715.
65. Roder, K., Wolf, S.S., Larkin, K.J. and Schweizer, M. (1999) Interaction between the two ubiquitously expressed transcription factors NF-Y and Sp1. *Gene*, **234**, 61–69.
66. Yamada, K., Tanaka, T., Miyamoto, K. and Noguchi, T. (2000) Sp family members and nuclear factor-Y cooperatively stimulate transcription from the rat pyruvate kinase M gene distal promoter region via their direct interactions. *J. Biol. Chem.*, **275**, 18129–18137.
67. Bandyopadhyay, S., Chiang, C.Y., Srivastava, J., Gersten, M., White, S., Bell, R., Kurschner, C., Martin, C., Smoot, M., Sahasrabudhe, S. et al. (2010) A human MAP kinase interactome. *Nat. Methods*, **7**, 801–805.
68. Kolell, K.J. and Crawford, D.L. (2002) Evolution of Sp transcription factors. *Mol. Biol. Evol.*, **19**, 216–222.
69. Li, X.Y., Hoof van Huijsduijnen, R., Mantovani, R., Benoist, C. and Mathis, D. (1992) Intron-exon organization of the NF-Y genes. Tissue-specific splicing modifies an activation domain. *J. Biol. Chem.*, **267**, 8984–8990.
70. Ge, Y., Jensen, T.L., Matherly, L.H. and Taub, J.W. (2002) Synergistic regulation of human cystathionine-beta-synthase-1b promoter by transcription factors NF-YA isoforms and Sp1. *Biochim. Biophys. Acta.*, **1579**, 73–80.
71. Choi, N.M. and Boss, J.M. (2012) Multiple histone methyl and acetyltransferase complex components bind the HLA-DRA gene. *PLoS One*, **7**, e37554.
72. Caretti, G., Cocchiarella, F., Sidoli, C., Villard, J., Peretti, M., Reith, W. and Mantovani, R. (2000) Dissection of functional NF-Y-RFX cooperative interactions on the MHC class II Ea promoter. *J. Mol. Biol.*, **302**, 539–552.

73. Hiscott, J. (2007) Triggering the innate antiviral response through IRF-3 activation. *J. Biol. Chem.*, **282**, 15325–15329.
74. Penkov, D., Mateos San Martín, D., Fernandez-Díaz, L.C., Rosselló, C.A., Torroja, C., Sánchez-Cabo, F., Warnatz, H.J., Sultan, M., Yaspo, M.L., Gabrieli, A. *et al.* (2013) Analysis of the DNA-binding profile and function of TALE homeoproteins reveals their specialization and specific interactions with Hox genes/proteins. *Cell Rep.*, **3**, 1321–1333.
75. Giannopoulou, E.G. and Elemento, O. (2013) Inferring chromatin-bound protein complexes from genome-wide binding assays. *Genome Res.*, **23**, 1295–1306.
76. Imbriano, C., Gnesutta, N. and Mantovani, R. (2012) The NF-Y/p53 liaison: well beyond repression. *Biochim. Biophys. Acta*, **1825**, 131–139.
77. Liberati, C., di Silvio, A., Ottolenghi, S. and Mantovani, R. (1999) NF-Y binding to twin CCAAT boxes: role of Q-rich domains and histone fold helices. *J. Mol. Biol.*, **285**, 1441–1455.
78. Bieda, M., Xu, X., Singer, M.A., Green, R. and Farnham, P.J. (2006) Unbiased location analysis of E2F1-binding sites suggests a widespread role for E2F1 in the human genome. *Genome Res.*, **16**, 595–605.
79. Müller, G.A. and Engeland, K. (2010) The central role of CDE/CHR promoter elements in the regulation of cell cycle-dependent gene transcription. *FEBS J.*, **277**, 877–893.
80. Chen, X., Müller, G.A., Quaa, M., Fischer, M., Han, N., Stutchbury, B., Sharrocks, A.D. and Engeland, K. (2013) The forkhead transcription factor FOXM1 controls cell cycle-dependent gene expression. *Mol. Cell. Biol.*, **33**, 227–236.
81. Tronche, F., Rollier, A., Herbomel, P., Bach, I., Cereghini, S., Weiss, M. and Yaniv, M. (1990) Anatomy of the rat albumin promoter. *Mol. Biol. Med.*, **7**, 173–185.
82. Milos, P.M. and Zaret, K.S. (1992) A ubiquitous factor is required for C/EBP-related proteins to form stable transcription complexes on an albumin promoter segment in vitro. *Genes Dev.*, **6**, 991–1004.
83. Shi, X., Metges, C.C. and Seyfert, H.M. (2012) Interaction of C/EBP-beta and NF-Y factors constrains activity levels of the nutritionally controlled promoter IA expressing the acetyl-CoA carboxylase-alpha gene in cattle. *BMC Mol. Biol.*, **13**, 21.
84. Su, M., Bansal, A.K., Mantovani, R. and Sodek, J. (2005) Recruitment of nuclear factor Y to the inverted CCAAT element (ICE) by c-Jun and E1A stimulates basal transcription of the bone sialoprotein gene in osteosarcoma cells. *J. Biol. Chem.*, **280**, 38365–38375.
85. Alonso, C.R., Pesce, C.G. and Kornblihtt, A.R. (1996) The CCAAT-binding proteins CP1 and NF-I cooperate with ATF-2 in the transcription of the fibronectin gene. *J. Biol. Chem.*, **271**, 22271–22279.
86. Yoshida, H., Okada, T., Haze, K., Yanagi, H., Yura, T., Negishi, M. and Mori, K. (2000) ATF6 activated by proteolysis binds in the presence of NF-Y (CBF) directly to the cis-acting element responsible for the mammalian unfolded protein response. *Mol. Cell. Biol.*, **20**, 6755–6767.
87. Yoshida, H., Okada, T., Haze, K., Yanagi, H., Yura, T., Negishi, M. and Mori, K. (2001) Endoplasmic reticulum stress-induced formation of transcription factor complex ERSF including NF-Y (CBF) and activating transcription factors 6alpha and 6beta that activates the mammalian unfolded protein response. *Mol. Cell. Biol.*, **21**, 1239–1248.
88. Luo, R., Lu, J.F., Hu, Q. and Maity, S.N. (2008) CBF/NF-Y controls endoplasmic reticulum stress induced transcription through recruitment of both ATF6(N) and TBP. *J. Cell. Biochem.*, **104**, 1708–1723.
89. Hollenhorst, P.C., McIntosh, L.P. and Graves, B.J. (2011) Genomic and biochemical insights into the specificity of ETS transcription factors. *Annu. Rev. Biochem.*, **80**, 437–471.
90. Göke, J., Chan, Y.S., Yan, J., Vingron, M. and Ng, H.H. (2013) Genome-wide kinase-chromatin interactions reveal the regulatory network of ERK signaling in human embryonic stem cells. *Mol. Cell.*, **50**, 844–855.
91. Yajima, H., Motohashi, N., Ono, Y., Sato, S., Ikeda, K., Masuda, S., Yada, E., Kanesaki, H., Miyagoe-Suzuki, Y., Takeda, S. *et al.* (2010) Six family genes control the proliferation and differentiation of muscle satellite cells. *Exp. Cell Res.*, **316**, 2932–2944.
92. Himeda, C.L., Ranish, J.A. and Hauschka, S.D. (2008) Quantitative proteomic identification of MAZ as a transcriptional regulator of muscle-specific genes in skeletal and cardiac myocytes. *Mol. Cell. Biol.*, **28**, 6521–6535.
93. Fan, W., Jin, S., Tong, T., Zhao, H., Fan, F., Antinore, M.J., Rajasekaran, B., Wu, M. and Zhan, Q. (2002) BRCA1 regulates GADD45 through its interactions with the OCT-1 and CAAT motifs. *J. Biol. Chem.*, **277**, 8061–8067.
94. Li, X., Liu, L., Yang, S., Song, N., Zhou, X., Gao, J., Yu, N., Shan, L., Wang, Q., Liang, J. *et al.* (2014) Histone demethylase KDM5B is a key regulator of genome stability. *Proc. Natl. Acad. Sci. U.S.A.*, **111**, 7096–7101.
95. Frontini, M., Imbriano, C., diSilvio, A., Bell, B., Bogni, A., Romier, C., Moras, D., Tora, L., Davidson, I. and Mantovani, R. (2002) NF-Y recruitment of TFIID, multiple interactions with histone fold TAF(II)s. *J. Biol. Chem.*, **277**, 5841–5848.
96. Kabe, Y., Yamada, J., Uga, H., Yamaguchi, Y., Wada, T. and Handa, H. (2005) NF-Y is essential for the recruitment of RNA polymerase II and inducible transcription of several CCAAT box-containing genes. *Mol. Cell. Biol.*, **25**, 512–522.
97. Biswas, M. and Chan, J.Y. (2010) Role of Nrf1 in antioxidant response element-mediated gene expression and beyond. *Toxicol. Appl. Pharmacol.*, **244**, 16–20.
98. Benatti, P., Dolfini, D., Viganò, A., Ravo, M., Weisz, A. and Imbriano, C. (2011) Specific inhibition of NF-Y subunits triggers different cell proliferation defects. *Nucleic Acids Res.*, **39**, 5356–5368.
99. Kidder, B.L., Hu, G. and Zhao, K. (2014) KDM5B focuses H3K4 methylation near promoters and enhancers during embryonic stem cell self-renewal and differentiation. *Genome Biol.*, **15**, R32.
100. Tyagi, S., Chabes, A.L., Wysocka, J. and Herr, W. (2007) E2F activation of S phase promoters via association with HCF-1 and the MLL family of histone H3K4 methyltransferases. *Mol. Cell.*, **27**, 107–119.
101. Zargar, Z. and Tyagi, S. (2012) Role of host cell factor-1 in cell cycle regulation. *Transcription*, **3**, 187–192.
102. Yang, M., Gocke, C.B., Luo, X., Borek, D., Tomchick, D.R., Machius, M., Otwinowski, Z. and Yu, H. (2006) Structural basis for CoREST-dependent demethylation of nucleosomes by the human LSD1 histone demethylase. *Mol. Cell.*, **23**, 377–387.
103. Cai, C., He, H.H., Gao, S., Chen, S., Yu, Z., Gao, Y., Chen, S., Chen, M.W., Zhang, J., Ahmed, M. *et al.* (2014) Lysine-Specific Demethylase 1 has dual functions as a major regulator of Androgen Receptor transcriptional activity. *Cell Rep.*, **9**, 1618–1627.
104. Flanagan, J.F., Mi, L.Z., Chruszcz, M., Cymborowski, M., Clines, K.L., Kim, Y., Minor, W., Rastinejad, F. and Khorasanizadeh, S. (2005) Double chromodomains cooperate to recognize the methylated histone H3 tail. *Nature*, **438**, 1181–1185.
105. Pray-Grant, M.G., Daniel, J.A., Schieltz, D., Yates, J.R. III and Grant, P.A. (2005) Chd1 chromodomain links histone H3 methylation with SAGA- and SLIK-dependent acetylation. *Nature*, **433**, 434–438.